



Cronfa - Swansea University Open Access Repository

This is an author produced version of a paper published in :

Quaternary Geochronology

Cronfa URL for this paper:

<http://cronfa.swan.ac.uk/Record/cronfa24276>

Paper:

Abbott, P., Bourne, A., Purcell, C., Davies, S., Scourse, J. & Pearce, N. (2015). Last Glacial Period Cryptotephra Deposits in an Eastern North Atlantic Marine Sequence: Exploring Linkages to the Greenland Ice-Cores. *Quaternary Geochronology*

<http://dx.doi.org/10.1016/j.quageo.2015.11.001>

This article is brought to you by Swansea University. Any person downloading material is agreeing to abide by the terms of the repository licence. Authors are personally responsible for adhering to publisher restrictions or conditions. When uploading content they are required to comply with their publisher agreement and the SHERPA RoMEO database to judge whether or not it is copyright safe to add this version of the paper to this repository.

<http://www.swansea.ac.uk/iss/researchsupport/cronfa-support/>

Last Glacial Period Cryptotephra Deposits in an Eastern North Atlantic Marine Sequence: Exploring Linkages to the Greenland Ice- Cores

Abbott, P.M.*¹, Bourne, A.J.¹, Purcell, C.S.², Davies, S.M.¹, Scourse, J.D.², Pearce,
N.J.G.³

¹Department of Geography, College of Science, Swansea University, Singleton Park,
Swansea, SA2 8PP, UK

²School of Ocean Sciences, Bangor University, Menai Bridge, Anglesey, LL59 5AB,
UK

³Department of Geography and Earth Sciences, Aberystwyth University, Aberystwyth,
SY23 3DB, UK

*Corresponding author (p.abbott@swansea.ac.uk; +441792 604138)

Abstract

The establishment of a tephra framework for the Greenland ice-cores spanning the last glacial period, particularly between 25-45 ka b2k, provides strong potential for precisely correlating other palaeoclimatic records to these key archives. Tephra-based synchronisation allows the relative timing of past climatic changes recorded within different depositional environments and potential causal mechanisms to be assessed. Recent studies of North Atlantic marine records have demonstrated the potential of tracing cryptotephra horizons in these sequences and the development of protocols now allows a careful assessment of the isochronous nature of such horizons. Here we

report on tephrochronological investigations of a marine sequence retrieved from the Goban Spur, Eastern North Atlantic, covering ~25-60 ka b2k. Density and magnetic separation techniques and an assessment of potential transport and depositional mechanisms have identified three previously unknown isochronous tephra horizons along with deposits of the widespread North Atlantic Ash Zone II and Faroe Marine Ash Zone III. Correlations between the new horizons and the Greenland ice-core tephra framework are explored and despite no tie-lines being identified the key roles that high-resolution climatostratigraphy and shard-specific trace element analysis can play within the assessment of correlations is demonstrated. The previously unknown horizons are new additions to the overall North Atlantic tephra framework for the last glacial period and could be key horizons for future correlations.

Keywords: Tephrochronology; palaeoclimate synchronisation; volcanic ash; isochrons; Iceland; major and trace element geochemistry

1. Introduction

The tracing of isochronous horizons of volcanic ash between different depositional realms (tephrochronology) has considerable potential for the independent correlation and synchronisation of disparate palaeoclimatic sequences and for assessing the relative timing of past climatic events (Lowe, 2011). The potential of tephrochronology to assess these relative timings is especially pertinent for the last glacial period as there is evidence for several abrupt climatic changes preserved within ice-cores from Greenland (e.g. GRIP Members, 1993; Johnsen et al., 2001; NGRIP Members, 2004) and numerous North Atlantic marine cores (e.g. Bond et al.,

1993, 1997; Van Kreveld et al., 2000; Martrat et al., 2007; Hall et al., 2011; Zumaque et al., 2012).

A large number of tephra horizons have been identified within multiple Greenland ice-cores spanning the last glacial period (Abbott and Davies, 2012; Bourne et al., 2013, 2015b; Davies et al., 2014). Bourne et al. (2015b) in particular increased the number of horizons identified in the NGRIP, NEEM, GRIP and DYE-3 ice-cores and, in combination with past studies, a framework of 99 geochemically characterised tephra deposits has now been defined for the 25-45 ka b2k period. Developing a framework of geochemically characterised horizons with strong stratigraphic and chronological control is an essential first step towards the synchronisation of these records to other palaeoclimatic sequences in a range of environments. A notable feature of the ice-core framework is the dominance of deposits, closely spaced in time, that have similar major element compositions relating to single sources, e.g. the Icelandic Grímsvötn volcanic system. Subtle major element differences can be used to discriminate between some deposits, but others have major element compositions which are indistinguishable (e.g. Bourne et al., 2013).

This compositional similarity presents a challenge when attempting to correlate tephra horizons from sequences with limited chronological and/or stratigraphic control. In these instances it has been widely advocated that any available climatostratigraphic evidence can be used alongside the compositional data to narrow down potential correlatives (e.g. Newnham and Lowe, 1999; Newnham et al., 2004; Pearce et al., 2008; Housley et al., 2012; MacLeod et al., 2015) and that trace element analysis of the tephra deposits may provide a useful secondary compositional fingerprint for

testing and assessing the robustness of correlations (e.g. Allan et al., 2008; Abbott et al., 2012, 2014; Albert et al., 2012; Lane et al., 2012; Bramham-Law et al., 2013; Pearce et al., 2014; Bourne et al., 2015a).

Overall, there is an order of magnitude difference between the number of tephra horizons identified in the Greenland ice-cores and North Atlantic marine sequences between 25-60 ka b2k. Only a few marine records have been investigated for their tephra content and there is a tendency to focus on visible horizons or on the coarse-grained components ($>150\text{ }\mu\text{m}$) (e.g. Lackschewitz and Wallrabe-Adams, 1997; Wastegård and Rasmussen, 2014). As a result, only two ice-marine tie-lines have been defined within the last glacial period. Firstly, the rhyolitic component of the widespread North Atlantic Ash Zone (NAAZ) II ($55,380 \pm 1184\text{ a b2k}$; Svensson et al., 2008) has been traced within multiple ice and marine cores (e.g. Kvamme et al., 1989; Grönvold et al., 1995; Lacasse et al., 1996; Zielinski et al., 1997; Haflidason et al., 2000; Austin et al., 2004). Secondly, Faroe Marine Ash Zone (FMAZ) II, a visible horizon identified in a number of marine cores from the Faroe Islands region (Wastegård et al., 2006), was traced into the NGRIP ice-core by Davies et al. (2008) (NGRIP 1848 m; $26,740 \pm 390\text{ a b2k}$). A third ice-marine correlation was also proposed between the NGRIP 2066.95 m horizon ($38,122 \pm 723\text{ a b2k}$) and FMAZ III, a thick and relatively scattered zone of glass shards traced between a number of the Faroe Islands region cores (Wastegård et al., 2006; Davies et al., 2010). However, Bourne et al. (2013) later highlighted the complexity of this period and identified a series of closely spaced tephra horizons with similar glass compositions in the NGRIP and NEEM ice-cores. Their compositions all fall within the broad compositional envelope of FMAZ III and the marine deposit has been interpreted as resulting from

the amalgamation of primary tephra-fall from a number of volcanic events as a consequence of low sedimentation rates at the marine core sites (Bourne et al., 2013; Griggs et al., 2014). Therefore, the prior correlation between FMAZ III and a single tephra layer in the ice-cores is no longer valid and should not be used as an ice-marine tie-line. However, the tephra layers in the ice may still act as tie-lines if individual homogenous horizons from those single events can be found in marine records. This particular example highlights some of the complexities involved with defining correlations between the records.

In recent years, there has been a shift towards the investigation of the cryptotephra record preserved within marine sediments. Density and magnetic separation techniques, previously applied to terrestrial sequences, have recently been successfully used to extract fine-grained cryptotephra, preserved as discrete deposits of glass shards, from a number of cores around the North Atlantic (e.g. Abbott et al., 2011, 2013, 2014; Griggs et al., 2014; Davies et al., 2014). Magnetic separation techniques are particularly important for the identification of basaltic cryptotephra in North Atlantic marine records because of the dominance of basaltic tephra deposits within the Greenland tephra framework (Abbott and Davies, 2012; Bourne et al., 2013, 2015b). In addition to these methodological advances, Griggs et al. (2014) outlined a protocol which uses a range of indicators to determine the potential influence of transportation and depositional processes on the stratigraphic and temporal integrity of marine tephra deposits. To date, these methods and approaches have not been utilised to isolate cryptotephra in North Atlantic marine sequences covering the 25-60 ka b2k period. The Greenland tephra framework in particular, now

demonstrates the potential for tephrochronological synchronisation if common horizons can be identified.

Here we report on tephrochronological investigations of the 25-60 ka b2k period within a marine core retrieved from the Goban Spur area in the eastern North Atlantic (MD04-2820CQ). Potential correlations to the Greenland tephra framework are explored with new high-resolution proxy data from MD04-2820CQ used to help determine the stratigraphic position of the tephra horizons and trace element analysis is utilised as a secondary compositional fingerprint.

2. Materials and Methods

2.1 MD04-2820CQ

MD04-2820CQ was retrieved from the Goban Spur area (49°05.29'N; 13°25.90'W; Figure 1) and is a reoccupation of the OMEX-2K core site (see Hall and McCave, 1998a,b; Scourse et al., 2000; Haapaniemi et al., 2010). A Ca XRF record and a low-resolution record of the percentage abundance of the polar foraminiferal species *Neogloboquadrina pachyderma* (sinistral) (*Np(s)*) have been used to define a preliminary stratigraphy for the sequence between MIS 3-2. A number of Dansgaard-Oeschger events related to the Greenland Interstadial (GI) events in the Greenland ice-cores are recognised within this record (Figure 2; Rasmussen et al., 2014). Between 450-550 cm depth, high-resolution (up to 1 cm) records of *Np(s)* and ice rafted debris (IRD) concentrations (150 µm-1 mm fraction) were generated to provide

a more detailed stratigraphy between DO-12 and DO-8 to help constrain the tephra deposits within a climatic framework (Figure 6).

FIGURE 1

The tephra content of the core was initially investigated at a low-resolution (5 cm contiguous samples) between 250-650 cm depth. Intervals with distinct peaks in glass shard content above background levels were subsequently re-investigated at 1 cm resolution to refine their stratigraphic position (Figure 2).

FIGURE 2

2.2 Extraction of tephra-derived glass shards from marine sequences

From the 5 and 1 cm samples, 0.5 g sub-samples of freeze-dried marine sediments were immersed in 10% HCl overnight to remove carbonate material. Samples were then wet sieved using 125 and 80 μm test sieves and 25 μm nylon mesh. The 25-80 μm fraction was then density separated using sodium polytungstate prepared to the specific gravities of 2.3 and 2.5 g/cm^3 to split the material into the density fractions of $<2.3 \text{ g}/\text{cm}^3$, to remove biogenic material, 2.3-2.5 g/cm^3 , to isolate rhyolitic material, and $>2.5 \text{ g}/\text{cm}^3$ to isolate basaltic material (Turney, 1998). To further purify the $>2.5 \text{ g}/\text{cm}^3$ fraction it was magnetically separated using a Frantz Isodynamic Magnetic Separator. The methodology and conditions for magnetic separation are outlined in Griggs et al. (2014) and allow the separation of non-magnetic quartz material from any paramagnetic basaltic material. The $>125 \mu\text{m}$ and 80-125 μm grain-size fractions,

and the 2.3-2.5 g/cm³ and magnetic >2.5 g/cm³ density fractions, were mounted on microscope slides in Canada Balsam for optical microscopy to quantify their glass shard content.

2.3 Geochemical analysis of individual glass shards

Samples for geochemical analysis were prepared using the procedure outlined in Section 2.2. The fraction of interest was then mounted in epoxy resin on a 28 × 48 mm frosted microscope slide to prepare thin sections of the glass shards. This was achieved by grinding the material using decreasing grades of silicon carbide paper and then polishing the surface using 9, 6 and 1 µm diamond suspension.

Major element compositions of individual shards were determined using electron-probe micro-analysis (EPMA) at the Tephra Analytical Unit, University of Edinburgh, using a Cameca SX100 with five wavelength dispersive spectrometers. The operating conditions followed those outlined in Hayward (2012). Calibration was carried out using pure metals, synthetic oxides and silicate standards and the secondary standards of Cannetto Lami Lava, Lipari and BCR2g were analysed at regular intervals to monitor for instrumental drift and assess the precision and accuracy of analysed samples (see Table S18). For data comparison all analyses were normalised to an anhydrous basis, i.e. 100 % total oxides, but all raw data analyses are provided in the supplementary information (Tables S1-S17). Statistical comparisons between tephra horizons have been made using the statistical distance test (D^2) of Perkins et al. (1995, 1998) and the similarity coefficient function (SC) of Borchardt et al. (1972).

Trace element compositions of single shards from one marine and one ice-core horizon were analysed using laser ablation inductively coupled plasma mass spectrometry (LA-ICP-MS) at Aberystwyth University. A Coherent GeoLas 193 nm Excimer laser coupled with a Thermo Finnigan Element 2 high-resolution sector field mass spectrometer was utilised (Pearce et al., 2011). Due to the small grain size of the shards making up the ice-core horizon, a laser with a beam diameter of 10 μm and a fluence of 10 J/cm^2 was pulsed at 5 Hz with a flash duration of ~ 10 ns. Despite the larger grain size of shards in the marine horizon, a 10 μm laser beam diameter was used for all analyses to limit any differential impact of fractionation effects. As a potential correlation was being tested, the samples were analysed ‘side-by-side’ to limit any potential influence of instrumental differences between analytical periods (Pearce et al., 2014). Trace element concentrations were calculated using methods outlined in Pearce et al. (2007), with ^{29}Si previously determined through EPMA used as the internal standard and NIST 612 used as the calibration standard, taking concentrations from Pearce et al. (1997). A correction factor was used to remove bias in analyses caused by fractional effects (Pearce et al., 2011). Trace element concentrations for individual shards are provided in Table S19 and analyses of the secondary standards BCR2g and BHVO-2g are provided in Table S20.

3. Results

Of the 80 intervals investigated at low-resolution, 21 were selected for high-resolution analysis resulting in the processing of 105 1 cm samples. Figure 2 integrates low-resolution counts from intervals that were not reanalysed with the high-resolution counts. These overall shard profiles were employed to select 17 samples for

geochemical analysis (Figure 2). Overall, the record contains a number of distinct concentrations of brown glass shards and this type of shard is also present as a low background. There is a more consistent background of rhyolitic shards throughout the whole of the studied interval. Given the tephrostratigraphical record, the deposits are grouped into five periods and used as a basis to present results below. To determine the source of the glass shards, compositions are compared to glass and whole rock analyses to allow material to be assigned to Icelandic rock suites and specific volcanic systems.

3.1 Period 1 - Post DO-3

Between 275-279 cm a dispersed zone of shards with a low concentration of basaltic shards and no discernible peak was identified. Geochemical characterisation shows that the glass in this zone has a highly heterogeneous composition with shards of both transitional alkali and tholeiitic composition present (Figure 3a). Similar heterogeneity is observed in shards from both the less-than and greater-than 80 μm grain-size fractions (Figure 3). This characterisation shows that the deposit is an amalgamation of material from a number of volcanic eruptions from multiple volcanic centres.

FIGURE 3

According to the stratigraphy for MD04-2820CQ, this zone of ash was deposited during the stadial period following DO-3. In the NGRIP ice-core, FMAZ II was deposited within Greenland Stadial (GS) 3 approximately 1000 years after the cooling

transition at the end of GI-3 (Davies et al., 2008). The composition of MD04-2820CQ 275-279 cm demonstrates that this deposit does not directly relate to the homogenous transitional alkali basaltic FMAZ II horizon found within ice and marine sequences (Figure 3b). Some shard analyses fall within the compositional envelopes of the homogenous VZ 1x and the heterogeneous VZ 1 ash zones from cores on the Reykjanes Ridge, but the greater heterogeneity of the 275-279 cm deposit suggests they are unrelated (Figure 3b).

The compositional heterogeneity and lack of a distinct peak in the shard concentration profile strongly suggests that this deposit represents a minor input of material, potentially through iceberg rafting or secondary transportation processes such as bottom currents, and cannot be regarded as isochronous.

3.2 Period 2 – DO-5 to DO-3

The highest glass shard concentration peak in the 25-80 μm fraction is observed within period 2 at 342-343 cm (Figure 2). The maximum peak in the $>125 \mu\text{m}$ size fraction is between 341-342 cm. Two narrow zones of ash below this high peak between 355-360 cm and 370-375 cm depth were found in low-resolution counts, but no distinct peaks in concentration were observed in the high-resolution counts.

Shards from the main peak and the two underlying ash zones have a basaltic composition (Figure 4a). With the exception of a shard population $>80 \mu\text{m}$ in size in the 373-374 cm sample, and a few outlying analyses that have affinities to the Icelandic transitional alkali rock suite, these deposits have a tholeiitic composition

sourced from the Kverkfjöll volcanic system (Figure 4a). Although the analysed glass shards are from four different depths, it is clear that the majority of shards from each interval occupy the same compositional space on geochemical plots and hence are related to one another. The relatively homogenous dominant population has SiO₂ concentrations between 48.5-51.0 %wt, CaO concentrations between 8.9-9.9 %wt and FeO concentrations of ~15 %wt (Figure 4). Slight geochemical bimodality can be observed, most notably within the TiO₂ concentrations and FeO/MgO ratios (Figure 4bi). This bimodality is present within the main shard peak at 342-343 cm and the underlying zones of low shard concentration. However, the deposit at 373-374 cm has proportionally more shards with high TiO₂ values than the other two deposits (Figure 4bi).

FIGURE 4

Determining potential correlatives, the isochronous nature and likely transport mechanisms for these deposits is complex. Bourne et al. (2015b) identified a number of tholeiitic basaltic tephra horizons with a Kverkfjöll source in the Greenland ice-cores between GI-5.2 and GS-4. The composition of all 10 of these ice-core horizons fall within the compositional field of the main population of the 342-343 cm and underlying deposits (Figure 4b), hampering their correlation to individual ice-core horizons. Some of these eruptives, however, have greater compositional heterogeneity, such as GRIP 2064.35 m, NGRIP 1931.60 m and NGRIP 1950.50 m, and cover the full compositional range observed in the marine deposit (Figure 4c). The peak input of ash at 342-343 cm may represent a single primary tephra-fall event related to one of these eruptions with the underlying deposits, between 355-360 and

370-375 cm, possibly representing downward movement of tephra within the sediment column via bioturbation. This scenario seems unlikely, however, due to the lack of a distinct background of basaltic shards between the deposits. An alternative scenario is that the geochemical similarities are a consequence of the marine deposits being composed of an amalgamation of glass shards from a number of eruptions. Shards could be amalgamated during protracted input of material via primary fall and post-depositional reworking, akin to the proposed depositional mechanism for FMAZ III (see Section 1). This proposition is, however, not supported by the relatively discrete nature of the peak input of ash to the site between 342-343 cm and the underlying deposits, which implies that tephra delivery occurred as short-lived pulses of material.

Delivery via repeated iceberg rafting events could create deposits of this nature. The greater heterogeneity of the material at 373-374 cm depth, with a transitional alkali composition similar to those of Katla eruptives in the Greenland tephra framework between GI-5.2 and GS-4 (Figure 4ai), and an additional tholeiitic population from Grímsvötn (Figure 4aii), may indicate that this material, with a slightly different compositional signature, is derived from a prior iceberg rafting event. We cannot fully test this proposition because an IRD record has currently not been established over this period. However, the high concentration of coarse-grained shards ($>125\ \mu\text{m}$) (Figure 2), in a relatively distal location to Iceland, supports iceberg rafting as the transport process. Overall, this likelihood prevents the deposits in period 2 from being useful regional isochrons but they could be used for local core correlations (Brendryen et al., 2010).

3.3 Period 3 – DO-9 to DO-8

Period 3 is characterised by an approximately 20 cm thick zone of elevated basaltic glass concentrations within which four small peaks in concentration can be observed. Peaks at 456-457 cm, 460-461 cm, 464-465 cm and 472-473 cm depth are observed in the 25-80 μm and >125 μm grain size fractions and three can be clearly observed in the 80-125 μm fraction. Each peak contains shards with affinities to either the transitional alkali or tholeiitic rock suites of Iceland, with the material from each of these rock suites displaying distinct heterogeneity (Figure 5a). Compositional similarities between the deposits and the continuous nature of the ash deposition allow the whole of the deposit between 455-475 cm to be interpreted as a single entity.

FIGURE 5

According to the MD04-2820CQ stratigraphy, this deposit spans the warming transition related to DO-8 (Figure 2 and 6), akin to the FMAZ III deposit identified in other North Atlantic marine records. Distinct similarities are evident between the heterogeneous Grímsvötn-sourced material of FMAZ III characterised from a record in the SE Norwegian Sea (Griggs et al., 2014) and the tholeiitic material present in this ash zone (Figure 5). Homogenous Grímsvötn-sourced populations identified in the Greenland tephra framework between GI-8c and GS-9 cannot be identified at any depth in MD04-2820CQ (Figure 7a). The geochemical range of the tholeiitic material in MD04-2820CQ encompasses that of glass in all the ice-core horizons (Figure 7a). Despite the failure to correlate to an ice-core deposit, the MD04-2820CQ deposit can be correlated to the marine FMAZ III due to the stratigraphic similarities and

geochemical affinity of the tholeiitic basaltic material. None of the Faroes Islands region occurrences of FMAZ III contain a population of transitional alkali material as observed in the MD04-2820CQ deposit (Figure 5; Wastegård et al., 2006; Griggs et al., 2014). Two transitional alkali basaltic horizons from Katla were identified in early GS-9 by Bourne et al. (2013, 2015b) and also fall within the range of the MD04-2820CQ analyses, but the heterogeneity is far greater in the marine deposits and no potential correlations can be suggested (Figure 7b).

FIGURE 6 AND 7

Griggs et al. (2014) interpreted FMAZ III in the Faroe Islands region as resulting from the amalgamation of primary fall material from closely timed Grímsvötn eruptions. Sediment accumulation rates are considered to be insufficient to allow the events to be separated and secondary processes such as bioturbation and bottom currents may have caused mixing of shards between depths. An ice-rafting transport and deposition mechanism was ruled out by Griggs et al. (2014) due to a lack of a coeval IRD signal. Within MD04-2820CQ, IRD concentrations are declining between 455-475 cm and there is no direct co-variance with glass shard concentrations (Figure 6). This lack of correlation could imply that the transport, deposition and post-deposition mechanisms are common between the MD04-2820CQ and JM11-FI-19PC core sites. The incorporation of transitional alkali material at the MD04-2820CQ site could result from more southerly transport of material from these eruptions. This would also account for the relative lack of transitional alkali eruptions in the Greenland tephra framework during this interval. As highlighted earlier, the FMAZ III cannot be used as a precise ice-marine tie-line (Bourne et al., 2013). However, the correlation of

MD04-2820CQ 455-475 cm to FMAZ III extends the geographical distribution of this deposit and it can be used as a marine-marine tie-line.

A small peak in colourless shards occurs at 463-464 cm and major element analysis shows that the glass has a rhyolitic composition and an affinity to the Icelandic transitional alkali rock suite (Figure 8a). Two populations are apparent, one with affinities to material from the rhyolitic component of NAAZ II and one with affinities to a number of Katla-sourced rhyolitic horizons deposited during the last glacial-interglacial transition and an underlying horizon in MD04-2820CQ at a depth of 497-498 cm (Figure 8b and c). These compositional affinities and the low shard concentration suggests that this material is not from a distinct volcanic event but may relate to a background of reworked colourless shards in the sequence.

FIGURE 8

3.4 Period 4 – DO-12 to DO-9

During this period a series of three relatively discrete peaks (~1-3 cm) in brown glass shards can be identified (Figure 2 and 6). The peaks in brown shards at 487-488 cm and 524-525 cm depth are distinct across all grain-size fractions, whereas the peak at 511-512 cm is only evident within the 25-80 and >125 µm grain-size fractions. A broad increase in colourless shards between 490-500 cm displays a double peak in concentration within the 25-80 µm grain-size fraction at 493-494 cm and 497-498 cm.

3.4.1 MD04-2820CQ 487-488 cm

399

400 All shards in the 487-488 cm deposit are basaltic in composition with one dominant
401 and homogenous tholeiitic population (Figure 9). Some outliers with a transitional
402 alkali composition are also observed, but are primarily restricted to the >80 μm
403 fraction (Figure 9a). The main population is characterised by SiO_2 concentrations of
404 ~49.5 %wt, TiO_2 concentrations between 2.6-3.2 %wt, CaO concentrations between
405 10.1 and 10.9 %wt and FeO concentrations of ~13.8 %wt, showing affinities to the
406 Grímsvötn volcanic system (Figure 9).

407

408 FIGURE 9

409

410 A large number of Grímsvötn eruptives are found within the Greenland tephra
411 framework between 25-45 ka b2k with several showing compositional similarities to
412 the main population of MD04-2820CQ 487-488 cm (Bourne et al., 2015b).
413 Stratigraphic information from MD04-2820CQ is thus employed to provide a broad
414 constraint on the timing of this eruption relative to the main climato-stratigraphic
415 framework for the North Atlantic. Further discussion of this approach is provided in
416 Section 4. MD04-2820CQ 487-488 cm was deposited just prior to Heinrich event 4
417 (Figure 6), which is widely regarded to have occurred in GS-9 and between DO-9 and
418 DO-8 (Sanchez Goñi and Harrison, 2010). The high-resolution $Np(s)$ record for this
419 interval shows that MD04-2820CQ 487-488 cm falls within a cold period above two
420 distinct decreases in $Np(s)$ percentages, between 490-510 cm depth, and thought to be
421 related to warming over the DO-9 and DO-10 events (Figure 6iii). These events were
422 not apparent within the original low resolution $Np(s)$ record or the Ca XRF record
423 (Figure 2ii and 6iv). These stratigraphic constraints suggest deposition during the cold

period following DO-9, which is equivalent to GS-9 within the Greenland stratigraphic framework (Rasmussen et al., 2014). The GS-9 interval has been fully sampled in all the ice-cores that contribute to the Greenland tephra framework (see Bourne et al., 2015b). In total, 10 Grímsvötn-sourced tephra horizons have been identified in one or more of the Greenland cores (Figure 6b). Geochemical comparisons show that no horizons provide a clear major element match to 487-488 cm. Therefore, a potential correlative to the marine horizon cannot be proposed (Figure 10a).

FIGURE 10

The transport mechanism for this deposit is unlikely to be iceberg rafting because of the relatively homogenous geochemical signature of the material and a lack of covariance with IRD (Figure 6). Other potential mechanisms, sea-ice rafting and primary airfall, would not impart a temporal delay and the deposit can be assumed to be isochronous. The relative proportion of larger grains in the 80-125 μm and $>125 \mu\text{m}$ fractions compared to other deposits, e.g. 524-525 cm, could be indicative of transportation via sea-ice rafting. This deposit is considered to have strong stratigraphic integrity as the peak in shard concentration is relatively discrete with only a restricted downward tail in concentration, most likely due to post-depositional bioturbation. Although not present in Greenland, if it was widely dispersed over the North Atlantic, this volcanic deposit may be a useful isochron for linking this sequence to other marine records.

3.4.2 MD04-2820CQ 493-494 cm and 497-498 cm

449

450 According to the stratigraphy for MD04-2820CQ, the slight increase in colourless
451 shards between 490-500 cm occurred during the short-lived cold period between DO-
452 10 and DO-9, based on an increase in $Np(s)$ percentages (Figure 2 and 6). Shards from
453 both peaks have a rhyolitic composition (Figure 8). The material from the larger peak
454 at 497-498 cm has affinities to the transitional alkali rock suite of Iceland and forms a
455 single homogenous population with SiO_2 concentrations between 70.5 and 71.5 %wt,
456 Al_2O_3 concentrations of ~13.5 %wt, K_2O concentrations of ~3.6 %wt and CaO
457 concentrations between 1.44 and 1.65 %wt (Figure 8). A source for these glass shards
458 could not be determined through comparisons to characterisations of proximal whole
459 rock rhyolites from Iceland, which may be due to the presence of other mineral phases
460 within whole rock analyses. However, compositional similarities to glass shards from
461 last glacial-interglacial transition rhyolitic tephra horizons sourced from the Katla
462 volcanic system (Figure 8b) strongly indicate that this is the volcanic source. Shards
463 in the overlying smaller peak at 493-494 cm fall into two populations, one with
464 affinities to the Katla material 4 cm below and one with strong overlap with shards
465 from 610-611 cm in the core from NAAZ II (Figure 8b and c). No rhyolitic horizons
466 have been isolated within the Greenland ice-core records between GI-9 and GI-11
467 (Bourne et al., 2015b).

468

469 The homogeneity of the 25 shards from the 497-498 cm peak and the predominance
470 of material in the 25-80 μm grain size fraction suggests that this represents primary
471 fall deposition. The upward tail in shard concentrations could be related to secondary
472 redistribution of material by bottom currents and the compositional bimodality in this
473 tail (493-494 cm sample) suggests reworking of the underlying Katla-sourced material

and NAAZ II input. Shards from NAAZ II (see Section 3.5) are present within overlying sediments and are the likely primary constituent of the reworked background of fine-grained rhyolitic material.

3.4.3 MD04-2820 CQ 511-512 cm

Brown shards from the peak at 511-512 cm are basaltic in composition with both tholeiitic and transitional alkali material present. Distinct heterogeneity can be observed in a number of components, e.g. Na₂O, K₂O, TiO₂ and FeO, and the analyses cannot be grouped into clear populations (Figure 9). The glass peak is directly associated with a peak in IRD, which combined with the geochemical signature strongly suggests it is an ice-rafted deposit and cannot be assumed to be isochronous.

3.4.4 MD04-2820 CQ 524-525 cm and 529-530 cm

The highest shard concentration in this period is found at 524-525 cm and exhibits a broader rise in shard concentrations including a small shard peak 4 cm below the main peak at 529-530 cm (Figure 2 and 6). The stratigraphy of MD04-2820CQ shows that the tephra horizon falls on the decrease in *Np(s)* percentage and increase in Ca content of the sediment that has been related to warming at the onset of DO-11 (Figure 2 and 6). Shards from both the main peak and underlying peak have a tholeiitic basaltic composition (Figure 9a). Shards from 524-525 cm form a homogenous population characterised by distinctly high FeO concentrations between 14.5 and 16.7 %wt, low CaO concentrations of ~9.25 %wt, TiO₂ concentrations of ~3.2 %wt and MgO

concentrations between 4.5 and 5.5 %wt (Figure 9). Comparison with proximal deposits highlights similarities to the products of both the Kverkfjöll and Grímsvötn volcanic systems (Figure 9b).

Four Grímsvötn-sourced deposits are found within the GS-12 climatic period and one within GI-11 in the Greenland tephra framework (Bourne et al., 2015b). Statistical comparisons show that none of these horizons are statistically different from 524-525 cm and all SC values exceed 0.95, due to the common source (Table 1). There is a clear affinity between the main population of MD04-2820CQ 524-525 cm and NGRIP 2162.05 m with a low D^2 value and the highest similarity coefficient of 0.977; this assessment is corroborated by major element biplot comparisons (Table 1; Figure 9b). To test this affinity, the trace element composition of both horizons was determined. Distinct differences can be observed in these characterisations, both in absolute concentrations and trace element ratios (Figure 10c). These demonstrate that the two horizons were not produced during the same volcanic event and cannot be correlated between the archives. The differences in trace element composition could be due to a number of factors, which will be discussed in Section 4.2.

TABLE 1

Assessing this deposit according to the protocol of Griggs et al. (2014) is problematic as key indicators are contradictory. The homogenous composition of the deposit suggests that this deposit was unlikely to be iceberg rafted, but it was deposited during a period of increased IRD concentrations (Figure 6). It is possible that primary fall deposition is superimposed on a period dominated by iceberg rafting. What is more,

iceberg rafting is typically thought to transport heterogeneous tephra deposits from an amalgamation of tephra from a number of eruptions. Tracing this horizon in the same stratigraphic position in another marine sequence would provide supporting evidence for this interpretation.

Glass shards from the small peak at 529-530 cm were additionally geochemically analysed to assess its relationship to the main overlying peak at 524-525 cm. All of the shards have a tholeiitic basaltic composition (Figure 9a), with three distinct major element populations present based on major oxides including FeO, CaO, MgO and Al₂O₃ (Figure 8bii). Half of the shards from this deposit make up the main population and indicate a source from either the Veidivötn-Bárdabunga or Reykjanes volcanic systems (Figure 9b). One population is sourced from Grímsvötn or Kverkfjöll and has compositional affinities to MD04-2820CQ 524-525 cm and the final population is sourced from Grímsvötn and has affinities to MD04-2820CQ 487-488 cm (Figure 9b). The only known tephra horizon in the Greenland ice-core framework between 25-45 ka b2k with a composition similar to the dominant population was deposited during GS-5 and thus is not a correlative to this deposit. The similarity in geochemistry between the sub-population and MD04-2820CQ 487-488 cm is likely to be coincidental, with the Greenland tephra framework showing that Grímsvötn produced many eruptives with similar compositions throughout this period (Bourne et al., 2015b). The heterogeneity of this material could be linked to some iceberg rafting of earlier events combined with downward reworking of material from the 524-525 cm peak.

3.5 Period 5 – DO-15 to DO-14

549

550 The highest concentration of colourless shards was observed at 610-611 cm with
551 ~19,500 shards per 0.5 g dry weight sediment (dws) in the 25-80 μm fraction and
552 ~450 shards in the $>125 \mu\text{m}$ fraction in this cryptotephra (Figure 2b). A peak in shards
553 80-125 μm in diameter associated with this deposit occurs 1 cm above this depth
554 between 609-610 cm (Figure 2b). Within the proposed MD04-2820CQ stratigraphy,
555 the shard concentration peak falls on the cooling transition at the end of DO-15 as
556 shown by the rise in the $Np(s)$ percentage (Figure 2b).

557

558 These colourless shards have a rhyolitic composition with affinities to the Icelandic
559 transitional alkali rock suite (Figure 8a) and are characterised by SiO_2 concentrations
560 of ~75.8 %wt, Al_2O_3 concentrations of ~11.7 %wt, FeO concentrations between 2.25
561 and 2.8 %wt and K_2O concentrations of ~4.2 %wt. Geochemical similarities are
562 highlighted between the MD04-2820CQ 610-611 cm deposit and other occurrences of
563 the rhyolitic component of NAAZ II (II-RHY-1) in North Atlantic marine sequences
564 and the GRIP ice-core (Figure 8c). There are some slight offsets between the MD04-
565 2820CQ characterisations and the older analyses, e.g. the MD04-2820CQ shards have
566 higher Na_2O and lower Al_2O_3 and SiO_2 concentrations, and these differences can be
567 attributed to the effect of sodium loss during the older analyses (Hunt and Hill, 2001;
568 Kuehn et al., 2011; Hayward, 2012). Therefore, these newer analyses represent a more
569 up-to-date characterisation of the II-RHY-1 component of NAAZ II and should be
570 utilised in future comparisons.

571

572 Identification of this horizon provides a direct ice-marine tie-line, a basal stratigraphic
573 constraint for the core, and a test of the proposed stratigraphy for MD04-2820CQ

because this horizon has been identified in the Greenland ice-cores and other marine sequences on the cooling transition at the end of GI-15 (Grönvold et al., 1995; Austin et al., 2004).

4. Discussion

4.1 Tephrostratigraphy of MD04-2820CQ between ~25-60 ka b2k and implications for the regional tephra framework

This work represents one of the first studies to employ density and magnetic separation techniques to isolate and identify cryptotephra within North Atlantic marine sediments between 25-60 ka b2k. Here, the identification of basaltic tephra deposits has been improved when compared with previous studies, e.g. Abbott et al. (2014), as magnetic separation of basaltic shards from the host sediment produced purer samples for optical microscopy work and geochemical analysis preparation.

Overall, the tephrostratigraphy of MD04-2820CQ is complex and differing transport and deposition processes have given rise to a range of contrasting deposits. For example, the geochemical heterogeneity of the MD04-2820CQ 275-279 cm and 511-512 cm deposits and to a certain extent the deposits between 340-380 cm depth suggests they were deposited via iceberg rafting. Whilst three of the deposits, the basaltic 487-488 cm and 524-525 cm and the rhyolitic 497-498 cm, have isochronous characteristics and have the potential to act as tie-lines between records, however none of these horizons were found to have correlatives within the current Greenland tephra framework (Table 2; see section 4.2 for further discussion).

599

600 TABLE 2

601

602 Two of the deposits in MD04-2820CQ have been correlated to previously known
603 tephra horizons (Table 2). MD04-2820CQ 610-611 cm correlates to NAAZ II and
604 permits a direct link to the Greenland ice-cores and other marine sequences while
605 MD04-2820CQ 455-475 cm can be correlated to FMAZ III, a broad marine-marine
606 link around DO-8 to sequences in the Faroe Island region. The MD04-2820CQ 455-
607 475 cm deposit differs from FMAZ III occurrences in the Faroe Islands region as it
608 contains transitional alkali basaltic glass in addition to the tholeiitic basaltic glass
609 characteristic of the original deposit (Griggs et al., 2014). Further work on tracing the
610 FMAZ III at sites between the Goban Spur area and the Faroe Islands region may help
611 isolate the transportation and depositional processes controlling this contrast. At
612 present the MD04-2820CQ core site on the Goban Spur is the furthest south that
613 FMAZ III has been identified; this increase in geographical range of the deposit
614 suggests that it could be a key stratigraphic marker for the DO-8 event in widespread
615 marine records.

616

617 The identification of horizons that do not at present have correlatives in other
618 palaeoarchives adds three further volcanic events into the regional framework for the
619 25-60 ka b2k period (Table 2). Tracing these horizons within other sequences would
620 test our assertion that these are atmospherically-derived and potentially validate their
621 use as isochronous tie-lines. This is most relevant for the MD04-2820CQ 497-498 cm
622 deposit which has a broader shard count profile relative to the two basaltic deposits.
623 The timing of emplacement of the three deposits can be inferred from their

relationship to the high-resolution stratigraphy for MD04-2820CQ shown in Figure 6, which can act as a guide for tracing these deposits in other records (Table 2).

The two basaltic deposits are thought to be sourced from the Grímsvötn and/or Kverkfjöll volcanic systems, providing further support for the high productivity of these systems during the last glacial period (cf. Bourne et al., 2015b). These results also demonstrate that their eruptive products were transported south of Iceland, most likely via direct atmospheric transport. Katla is thought to be the most likely source of MD04-2820CQ 497-498 cm and a correlative could not be identified in the Greenland ice-cores (Section 3.4.2; Bourne et al., 2015b). Indeed, no rhyolitic tephra horizons from this source and very few Icelandic rhyolitic horizons are present throughout the last glacial period in the Greenland ice-cores (Davies et al., 2014; Bourne et al., 2015b). The identification of this Katla horizon within the cool interval between DO-10 and DO-9 thus demonstrates that older rhyolitic eruptions from this source did occur prior to the last glacial-interglacial transition (Lane et al., 2012).

4.2 Testing correlations using stratigraphy and trace element analysis

The stratigraphy of MD04-2820CQ and its likely relationship to the Greenland climatic record was used throughout to assess the timing of the emplacement of the tephra deposits. This climatostratigraphic approach was particularly crucial for assessing potential correlatives for the MD04-2820CQ 487-488 cm and 524-525 cm horizons and high-resolution records of $Np(s)$ and IRD were available for these purposes.

649 The correlation of tephtras solely based on geochemical matches between horizons,
650 relies on every eruption having a unique geochemical signature. For the North
651 Atlantic region, however, the new Greenland tephra framework demonstrates that
652 multiple basaltic horizons with overlapping geochemical signatures were erupted
653 within relatively short time-intervals (Bourne et al., 2013, 2015b). Therefore, as is
654 required for many other tephrochronological studies, stratigraphic control was used
655 alongside the compositional data to guide the testing of correlations. This approach
656 does introduce an element of circularity if the tephra correlations are to be used as
657 climatically independent tools to test stratigraphic comparisons and the relative timing
658 of past climatic changes (see discussion in Matthews et al., 2015). However, in this
659 instance the approach is valid as the overall stratigraphy of MD04-2820CQ is
660 supported by distinct event markers such as Heinrich Event 4 and NAAZ II and there
661 is a strong relationship to the sequence of well-defined Greenland Interstadial events
662 recorded in the ice-cores. This relationship is especially apparent over the section
663 where high-resolution proxy data has been acquired. In addition, the stratigraphic
664 comparisons used to test correlations were broad and on a millennial-scale, and not
665 centennial or decadal-scale which is the potential magnitude of climatic phasing
666 between the environments.

667
668 The use of stratigraphy to guide correlations will be limited or problematic when
669 correlations are being assessed between the Greenland records and marine sequences
670 that have a less well-resolved stratigraphic framework, due to core location and/or
671 sedimentation rate differences. However, due to the high frequency of Icelandic
672 basaltic eruptions, particularly from Grímsvötn, some form of stratigraphic constraint
673 is essential for exploring potential tie-lines. We recommend that, when possible, high-

resolution stratigraphic information is gained over key intervals of interest to aid correlation testing.

The potential correlation between MD04-2820CQ and NGRIP 2162.05 m was tested using grain-specific trace element analysis, due to strong major element similarities (Figure 10b). This analysis showed that the two horizons were not produced during the same volcanic event (Figure 10c). The use of trace element analysis to test and add robustness to correlations has been encouraged previously and its use is steadily increasing within tephrochronological studies (see Section 1). Our work provides further support for the use of this technique for testing correlations and for providing a key insight into geochemical variability between Icelandic eruptions, specifically those sourced from the Grímsvötn volcanic system. As basaltic magmas have undergone relatively limited compositional evolution, intra-eruption variability in trace elements from a single evolving system could be limited as significant fractional crystallisation may not have occurred, this being the process which dominantly controls trace element evolution (see Pearce et al., 2008). Therefore, it is of interest to see clear trace element differences between two Grímsvötn-sourced eruptions with highly similar major element compositions. In this instance, the differences could result from magmatic evolution within a single, fractionating magma chamber between eruptions or the eruptions tapped magma from different fissures within the overall Grímsvötn system with similar major element but differing trace element compositions. Trace element analysis of proximal deposits could provide an insight into the intra-eruption variability of Grímsvötn basalts.

5. Conclusions

699

700 The potential for using density and magnetic separation techniques to identify tephra
701 deposits within North Atlantic marine sequences spanning ~25-60 ka b2k has been
702 clearly demonstrated. Applying these techniques to MD04-2820CQ has unearthed a
703 complex tephrostratigraphical record with differing transportation and depositional
704 processes operating at different times, but the identification of isochronous deposits
705 highlights the potential for using tephrochronology to link marine sequences. One of
706 the biggest challenges for establishing correlations is the high number of
707 compositionally similar eruptives preserved in the ice-cores within short time-
708 intervals. We have outlined how stratigraphic constraints can help reduce the number
709 of potential candidates and the need for high-resolution proxy data to constrain key
710 intervals. The use of stratigraphic constraints from proxy data could ultimately be
711 limited by the resolution of marine records. In addition, it has been shown that trace
712 element comparisons provide a secondary fingerprint that can test the robustness of
713 correlations suggested by major element geochemical similarities. Exploration of
714 further records in this region will help assess the isochronous nature of the key
715 deposits in MD04-2820CQ and represent a major step towards synchronisation of
716 regional marine archives using cryptotephra deposits.

717

718 **Acknowledgements**

719

720 PMA, AJB and SMD are financially supported by the European Research Council
721 (TRACE project) under the European Union's Seventh Framework Programme
722 (FP7/2007-2013) / ERC grant agreement no. [259253]. SMD is also partly supported
723 by a Philip Leverhulme Prize. Core MD04-2820CQ was acquired with support from

724 UK Natural Environment Research Council Standard Grant NER/A/S/2001/01189
725 (JDS). CSP acknowledges the support of a NERC PhD Training Support Grant
726 (NE/L501694/1). We would like to thank Dr Chris Hayward for his assistance with the
727 use of the electron microprobe at the Tephrochronology Analytical Unit, University of
728 Edinburgh. Thanks also to Gareth James, Gwydion Jones and Kathryn Lacey
729 (Swansea University) for laboratory assistance. Thanks to David Lowe for a thorough
730 and comprehensive review of the manuscript. This paper is a contribution to the
731 Climate Change Consortium of Wales (C3W). This paper contributes to the
732 INTREPID Tephra II (Enhancing tephrochronology as a global research tool through
733 improved fingerprinting and correlation techniques and uncertainty modelling: phase
734 II) – an INQUA INTAV-led project (International Focus Group on Tephrochronology
735 and Volcanism, project No. 1307s).

Figures

Figure 1: Location map of the MD04-2820CQ core site and other cores referred to within the text.

Figure 2: (a) Climate and tephrostratigraphy of the last glacial period within the MD04-2820CQ core. (i) XRF (ITRAX core scanning) Ca count rates (ii) percentage abundance of *Neogloboquadrina pachyderma* (sinistral) (iii) tephrostratigraphy incorporating 5 and 1 cm resolution shard counts. (b) Inset of climate and tephrostratigraphy of colourless shards between 550-650 cm depth. This figure is an expansion of the colourless shard counts that were truncated on Figure 2a. Red bars denote depth intervals from which glass shards were extracted for geochemical analysis.

Figure 3: Comparison of glass compositions from MD04-2820CQ 275-279 cm to that from FMAZ II, VZ 1x and VZ 1 characterisations from Davies et al. (2008), Griggs et al. (2014) and Lackschewitz and Wallrabe-Adams (1997). (a) Inset of total alkalis versus silica plot. Division line to separate alkaline and sub-alkaline material from MacDonald and Katsura (1964). Chemical classification and nomenclature after Le Maitre et al. (1989). (b) (i) CaO vs FeO and (ii) K₂O vs TiO₂ biplot comparisons. NGRIP data from Davies et al. (2008), JM11-19PC data from Griggs et al. (2014) and VZ 1x and VZ 1 data from Lackschewitz and Wallrabe-Adams (1997). All plots on a normalised anhydrous basis.

Figure 4: Compositional characterisation of MD04-2820CQ glass shard deposits between 340-380 cm depth, comparisons to proximal Icelandic deposits and comparisons with horizons with a Kverkfjöll volcanic source in the Greenland tephra framework. (a) (i) inset of total alkalis versus silica plot. Division line to separate alkaline and sub-alkaline material from MacDonald and Katsura (1964). Chemical classification and nomenclature after Le Maitre et al. (1989). (ii and iii) Compositional variation diagrams comparing analyses to deposits proximal to four tholeiitic Icelandic volcanic systems. Compositional fields defined using glass and whole rock analyses from Jakobsson et al. (2008) (Reykjanes), Höskuldsson et al. (2006) and Óladóttir et al. (2011) (Kverkfjöll) and Jakobsson (1979), Haflidason et al. (2000) and Óladóttir et al. (2011) (Grímsvötn and Veidivötn-Bardabunga). (b) (i) Compositional variation diagram of glass between 340-380 cm depth in MD04-2820CQ (ii) Compositional variation diagram of glass from ice-core horizons from the framework of Bourne et al. (2015b). (c) Compositional variation diagram of glass from MD04-2820CQ 342-343 cm and glass from three heterogeneous Kverkfjöll eruptives identified between GI-5.2 and GS-4 in the Greenland tephra framework of Bourne et al. (2015b). Ice-core horizons in bold are identified in multiple cores. All plots on a normalised anhydrous basis.

Figure 5: Compositional characterisation of glass from MD04-2820CQ tephra deposits between 455-475 cm depth and comparison to the glass characterised for FMAZ III. (a) inset of total alkali vs. silica plot. Division line to separate alkaline and sub-alkaline material from MacDonald and Katsura (1964). Chemical classification and nomenclature after Le Maitre et al. (1989). (b) Compositional variation diagrams

for tholeiitic glass. FMAZ III data from JM11-19PC core outlined in Griggs et al. (2014). All plots on a normalised anhydrous basis.

Figure 6: (a) High-resolution stratigraphy of the 450-550 cm interval within MD04-2820CQ. (i) Stratigraphy of colourless glass shard concentrations. (ii) Stratigraphy of brown glass shard concentrations. Red bars denote samples from which shards were extracted for compositional analysis. (iii) High-resolution percentage abundance of *Neogloboquadrina pachyderma* (sinistral). (iv) XRF (ITRAX core scanning) Ca count rates. (v) High-resolution IRD counts. Light green bars highlight glass shard peaks with homogenous compositions. (b) Greenland tephra framework between GI-8 and GI-12 (Bourne et al., 2015b and references within) plotted on the NGRIP oxygen isotope stratigraphy (NGRIP Members, 2004). Green lines denote horizons that can be traced in multiple cores. Other horizons are only present in NGRIP (red), NEEM (purple), GRIP (yellow) and DYE-3 (blue).

Figure 7: (a) Compositional comparisons of tholeiitic glass from MD04-2820CQ Period 3 deposits and GI-8c and GS-9 tephras in the Greenland tephra framework of Bourne et al. (2013, 2015b). (b) Compositional comparisons of transitional alkali glass from MD04-2820CQ Period 3 deposits and GS-9 tephras in the Greenland tephra framework. Ice-core data from Bourne et al. (2015b). Ice-core horizons in bold can be traced in multiple cores and only data from the NGRIP occurrence have been used for those horizons. All plots on a normalised anhydrous basis. The key for analyses from MD04-2820CQ is the same as Figure 5.

Figure 8: (a) Inset of total alkali vs. silica plot focusing on rhyolitic material from the MD04-2820CQ core. Normalised compositional fields for the Icelandic rock suites derived from whole rock analyses in Jakobsson et al. (2008). Chemical classification and nomenclature after Le Maitre et al. (1989). (b) Compositional variation diagrams comparing low SiO₂ rhyolitic glass from MD04-2820CQ to geochemical fields for a number of Katla-derived tephra horizons. Glass compositions from Lane et al. (2012) (Vedde Ash and Dimna Ash), Matthews et al. (2011) (AF555; Abernethy Tephra (MacLeod et al., 2015)) and Pilcher et al. (2005) (Suduroy). (c) Compositional variation diagrams comparing high SiO₂ rhyolitic glass from MD04-2820CQ to fields for marine and ice occurrences of the NAAZ II rhyolitic component. Glass data from Austin et al. (2004) (MD95-2006), Wastegård et al. (2006) (ENAM93-20, ENAM33, EW9302-2JPC), Brendryen et al. (2011) (SO82-05, MD99-2289) and Grönvold et al. (1995). All plots on a normalised anhydrous basis.

Figure 9: Compositional characterisation of basaltic glass from deposits between 485 and 530 cm in MD04-2820CQ and comparisons with Icelandic proximal material. (a) inset of inset of total alkali vs. silica plot. Division line to separate alkaline and sub-alkaline material from MacDonald and Katsura (1964). Chemical classification and nomenclature after Le Maitre et al. (1989). (b) Compositional variation diagrams comparing analyses with material proximal to four tholeiitic Icelandic volcanic systems. Compositional fields defined using glass and whole rock analyses from Jakobsson et al. (2008) (Reykjanes), Höskuldsson et al. (2006) and Óladóttir et al. (2011) (Kverkfjöll) and Jakobsson (1979), Haflidason et al. (2000) and Óladóttir et al. (2011) (Grímsvötn and Veidivötn-Bardabunga). All plots on a normalised anhydrous basis.

833

834 **Figure 10:** (a) Comparison of the main tholeiitic glass population of MD04-2820CQ
835 487-488 cm with glass compositional fields for GS-9 tephra horizons sourced from
836 Grímsvötn in the Greenland tephra framework of Bourne et al. (2015b). Horizons in
837 bold have been identified in multiple ice-cores. (b) Comparison of MD04-2820CQ
838 524-525 cm glass with characterisations of glass from tephra horizons in the
839 Greenland tephra framework of Bourne et al. (2015b). (c) Comparison of trace
840 element characterisations of individual shards from MD04-2820CQ 524-525 cm and
841 NGRIP 2162.05 m. All plots on a normalised anhydrous basis.

842

843 **Table 1:** Statistical comparisons of the main tholeiitic population of glass from
844 MD04-2820CQ 524-525 cm with glass from GI-11 and GS-12 tephra horizons within
845 the Greenland tephra framework. Some outliers were removed from the ice-core
846 characterisations. Critical value of 23.21 for statistical distance comparisons (10
847 degrees of freedom; 99 % confidence interval).

848

849 **Table 2:** Summary of tephra horizons in MD04-2820CQ with the potential to act as
850 widespread tie-lines to other palaeoclimatic sequences in the North Atlantic region.
851 The timing of events is based on the stratigraphy for the MD04-2820CQ record.

852 *Only to be used as a marine-marine tie-point.

853

References

- Abbott, P.M., Austin, W.E.N., Davies, S.M., Pearce, N.J.G., Hibbert, F.D., 2013. Cryptotephrochronology of a North East Atlantic marine sequence over Termination II, the Eemian and the last interglacial-glacial transition. *Journal of Quaternary Science* 28, 501-514.
- Abbott, P.M., Austin, W.E.N., Davies, S.M., Pearce, N.J.G., Rasmussen, T.L., Wastegård, S., Brendryen, J., 2014. Re-evaluation and extension of the MIS 5 tephrostratigraphy of the Faroe Islands Region: the cryptotephra record. *Palaeogeography, Palaeoclimatology, Palaeoecology* 409, 153-168.
- Abbott, P.M., Davies, S.M., 2012. Volcanism and the Greenland ice-cores: the tephra record. *Earth-Science Reviews* 115, 173-191.
- Abbott, P.M., Davies, S.M., Austin, W.E.N., Pearce, N.J.G., Hibbert, F.D., 2011. Identification of cryptotephra horizons in a North East Atlantic marine record spanning marine isotope stages 4 and 5a (~60,000-82,000 a b2k). *Quaternary International* 246, 177-189.
- Albert, P.G., Tomlinson, E.L., Smith, V.C., Di Roberto, A., Todman, A., Rosi, M., Marini, M., Muller, W., Menzies, M., 2012. Marine-continental tephra correlations: Volcanic glass geochemistry from the Marsili Basin and the Aeolian Islands, Southern Tyrrhenian Sea, Italy. *Journal of Volcanology and Geothermal Research* 229-230, 74-94.
- Allan, A.S.R., Baker, J.A., Carter, L., Wysoczanski, R.J., 2008. Reconstructing the Quaternary evolution of the world's most active silicic volcanic system: insights from an ~1.65 Ma deep ocean tephra record sourced from Taupo Volcanic Zone, New Zealand. *Quaternary Science Reviews* 27, 2341-2360.
- Austin, W.E.N., Wilson, L.J., Hunt, J.B., 2004. The age and chronostratigraphical significance of North Atlantic Ash Zone II. *Journal of Quaternary Science* 19, 137-146.
- Bond, G., Broecker, W., Johnsen, S., McManus, J., Labeyrie, L., Jouzel, J., Bonani, G., 1993. Correlations between climate records from North Atlantic sediments and Greenland ice. *Nature* 365, 143-147.
- Bond, G., Showers, W., Cheseby, M., Lotti, R., Almasi, P., deMenocal, P., Priore, P., Cullen, H., Hajdas, I., Bonani, G., 1997. A Pervasive Millennial-Scale Cycle in North Atlantic Holocene and Glacial Climates. *Science* 278, 1257-1266.
- Borchardt, G.A., Aruscavage, P.J., Millard, H., 1972. Correlation of the Bishop ash, a Pleistocene marker bed, using instrumental neutron activation analysis. *Journal of Sedimentary Petrology* 42, 201-206.
- Bourne, A., Albert, P.G., Matthews, I.P., Trincardi, F., Wulf, S., Asioli, A., Blockley, S.P.E., Keller, J., Lowe, J.J., 2015a. Tephrochronology of core PRAD 1-2 from the

Adriatic Sea: insights into Italian explosive volcanism for the period 200-80 ka. Quaternary Science Reviews 116, 28-43.

Bourne, A.J., Cook, E., Abbott, P.M., Seierstad, I.K., Steffensen, J.P., Svensson, A., Fischer, H., Schupbach, S., Davies, S.M., 2015b. A tephra lattice for Greenland and a reconstruction of volcanic events spanning 25-45 ka b2k. Quaternary Science Reviews 118, 122-141.

Bourne, A.J., Davies, S.M., Abbott, P.M., Rasmussen, S.O., Steffensen, J.P., Svensson, A., 2013. Revisiting the Faroe Marine Ash Zone III in two Greenland ice cores: implications for marine-ice correlations. Journal of Quaternary Science 28, 641-646.

Bramham-Law, C.W.F., Theuerkauf, M., Lane, C.S., Mangerud, J., 2013. New findings regarding the Saksunarvatn Ash in Germany. Journal of Quaternary Science 28, 248-257.

Brendryen, J., Haflidason, H., Sejrup, H.P., 2010. Norwegian Sea tephrostratigraphy of marine isotope stages 4 and 5: Prospects and problems for tephrochronology in the North Atlantic region. Quaternary Science Reviews 29, 847-864.

Brendryen, J., Haflidason, H., Sejrup, H.P., 2011. Non-synchronous deposition of North Atlantic Ash Zone II in Greenland ice cores, and North Atlantic and Norwegian Sea sediments: an example of complex glacial-stage tephra transport. Journal of Quaternary Science 26, 739-745.

Davies, S.M., Abbott, P.M., Meara, Rh. H., Pearce, N.J.G., Austin, W.E.N., Chapman, M. R., Svensson, A., Bigler, M., Rasmussen, T.L., Rasmussen, S.O., Farmer, E.J., 2014. A North Atlantic tephrostratigraphical framework for 130-60 ka b2k: new tephra discoveries, marine-based correlations, and future challenges. Quaternary Science Reviews 106, 101-121.

Davies, S.M., Wastegård, S., Abbott, P.M., Barbante, C., Bigler, M., Johnsen, S.J., Rasmussen, T.L., Steffensen, J.P., Svensson, A., 2010. Tracing volcanic events in the NGRIP ice-core and synchronising North Atlantic marine records during the last glacial period. Earth and Planetary Science Letters 294, 69-79.

Davies, S.M., Wastegård, S., Rasmussen, T.L., Svensson, A., Johnsen, S.J., Steffensen, J.P., Andersen, K.K., 2008. Identification of the Fugloyarbanki tephra in the NGRIP ice core: a key tie-point for marine and ice-core sequences during the last glacial period. Journal of Quaternary Science 23, 409-414.

Greenland Ice-core Project (GRIP) Members, 1993. Climate instability during the last interglacial period recorded in the GRIP ice core. Nature 364, 203-207.

Griggs, A.J., Davies, S.M., Abbott, P.M., Rasmussen, T.L., Palmer, A.P., 2014. Optimising the use of marine tephrochronology in the North Atlantic: A detailed investigation of the Faroe Marine Ash Zones II, III and IV. Quaternary Science Reviews 106, 122-139.

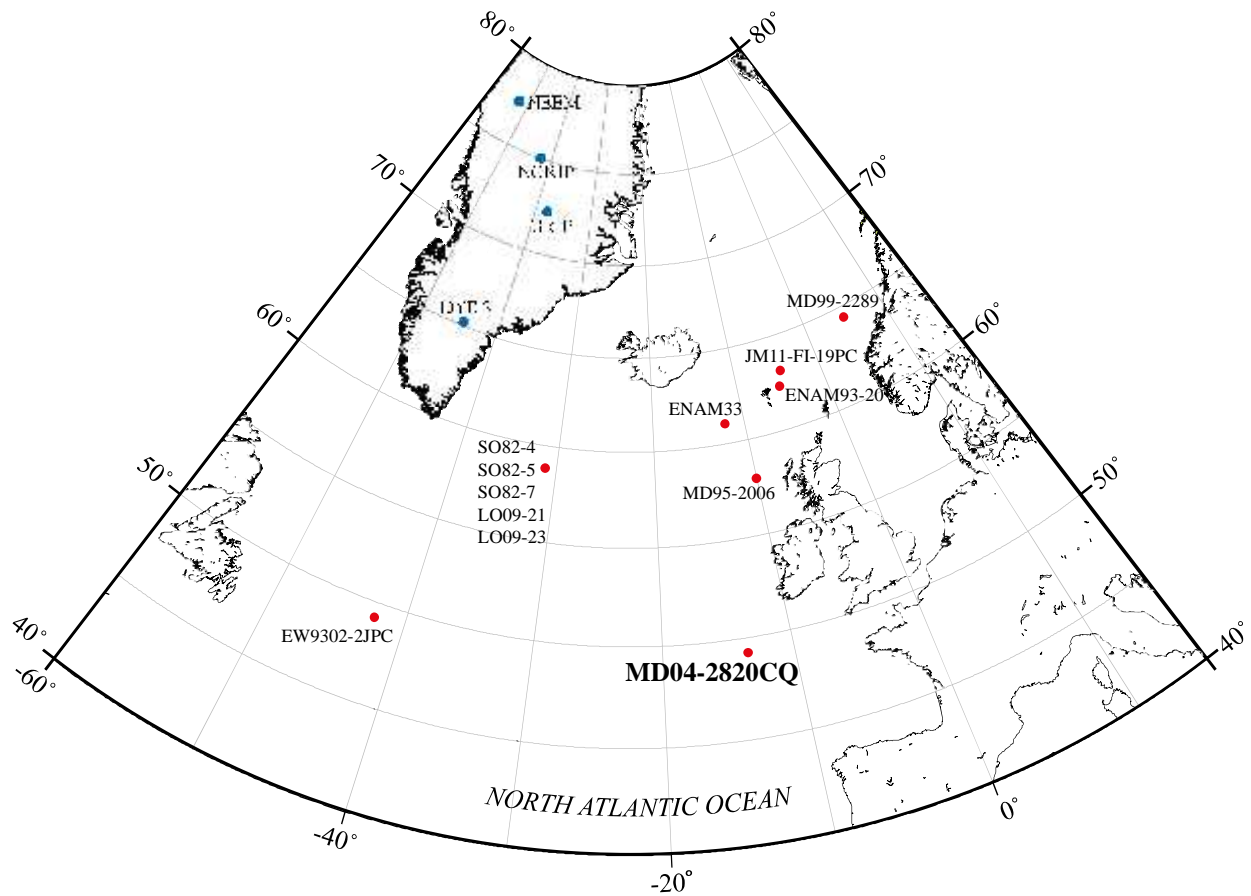
953 Grönvold K., Óskarsson N., Johnsen S.J., Clausen H.B., Hammer C.U., Bond G.,
 954 Bard E., 1995. Ash layers from Iceland in the Greenland GRIP ice core correlated
 955 with oceanic and land sediments. *Earth and Planetary Science Letters* 135, 149-155.
 956
 957 Haapaniemi, A.I., Scourse, J.D., Peck, V.L., Kennedy, H., Kennedy, P., Hemming,
 958 S.R., Furze, M.F.A., Pie kowski, A.J., Austin, W.E.N., Walden, J., Wadsworth, E.,
 959 Hall, I.R., 2010. Source, timing, frequency and flux of ice-rafted detritus to the
 960 Northeast Atlantic margin, 30-12 ka: testing the Heinrich precursor hypothesis.
 961 *Boreas* 39, 576-591.
 962
 963 Haflidason H., Eiriksson J., Van Kreveld S., 2000. The tephrochronology of Iceland
 964 and the North Atlantic region during the Middle and Late Quaternary: a review.
 965 *Journal of Quaternary Science* 15, 3-22.
 966
 967 Hall, I.R., Colmenero-Hidalgo, E., Zahn, R., Peck, V.L., Hemming, S.R., 2011.
 968 Centennial- to millennial-scale ice-ocean interactions in the subpolar northeast
 969 Atlantic 18-41 kyr ago. *Paleoceanography* 26, PA2224, doi:10.1029/2010PA002084.
 970
 971 Hall, I.R., McCave, I.N., 1998a. Late Glacial to recent accumulation fluxes of
 972 sediments at the shelf edge and slope of NW Europe, 48-50°N. *Special Publications of*
 973 *the Geological Society of London* 129, 339-350.
 974
 975 Hall, I.R., McCave, I.N., 1998b. Glacial-interglacial variation in organic carbon burial
 976 on the slope of the NW European continental margin (40°-50°N). *Progress in*
 977 *Oceanography* 42, 37-60.
 978
 979 Hayward, C., 2012. High spatial resolution electron probe microanalysis of tephras
 980 and melt inclusions without beam-induced chemical modification. *The Holocene* 22,
 981 119-125.
 982
 983 Höskuldsson, Á., Sparks, R.S.J., Carroll, M.R., 2006. Constraints on the dynamics of
 984 subglacial basalt eruptions from geological and geochemical observations at
 985 Kverkfjöll, NE-Iceland. *Bulletin of Volcanology* 68, 689-701.
 986
 987 Housley, R.A., Lane, C.S., Cullen, V.L., Weber, M.-J., Riede, F., Gamble, C.S.,
 988 Brock, F., 2012. Icelandic volcanic ash from the Late-glacial open-air archaeological
 989 site of Ahrenshöft LA 58 D, North Germany. *Journal of Archaeological Science* 39,
 990 708-716.
 991
 992 Hunt, J.B., Hill, P.G., 2001. Tephrological implications of beam size-sample-size
 993 effects in electron microprobe analysis of glass shards. *Journal of Quaternary Science*
 994 16, 105-117.
 995
 996 Jakobsson, S.P., 1979. Petrology of recent basalts of the Eastern Volcanic Zone,
 997 Iceland. *Acta Naturalia Islandia* 26, 1-103.
 998
 999 Jakobsson, S.P., Jónasson, K., Sigurdsson, I.A., 2008. The three igneous rock suites of
 1000 Iceland. *Jökull* 58, 117-138.
 1001
 1002 Johnsen, S.J., Dahl-Jensen, D., Gundestrup, N., Steffensen, J.P., Clausen, H.B.,

- Miller, H., Masson-Delmotte, V., Sveinbjörnsdóttir, A.E., White, J., 2001. Oxygen isotope and palaeotemperature records from six Greenland ice-core stations: Camp Century, Dye-3, GRIP, GISP2, Renland and NorthGRIP. *Journal of Quaternary Science* 16, 299-307.
- Kuehn, S.C., Froese, D.G., Shane, P.A.R., INTAV Intercomparison Participants (2011) "The INTAV intercomparison of electron-beam microanalysis of glass by tephrochronology laboratories: Results and recommendations", *Quaternary International* 246, 19-47.
- Kvamme T., Mangerud J., Furnes H., Ruddiman W., 1989. Geochemistry of Pleistocene ash zones in cores from the North Atlantic. *Norsk Geologisk Tidsskrift* 69, 251-272.
- Lacasse C., Sigurdsson H., Carey S., Paterne M., Guichard F., 1996. North Atlantic deep-sea sedimentation of Late Quaternary tephra from the Iceland hotspot. *Marine Geology* 129, 207-235.
- Lackschewitz, K.S., Wallrabe-Adams, H.J., 1997. Composition and origin of volcanic ash zones in Late Quaternary sediments from the Reykjanes Ridge: evidence for ash fallout and ice-rafting. *Marine Geology* 136, 209-224.
- Lane, C.S., Blockley, S.P.E., Mangerud, J., Smith, V.C., Lohne, Ø.S., Tomlinson, E.L., Matthews, I.P., Lotter, A.F., 2012. Was the 12.1 ka Icelandic Vedde Ash one of a kind? *Quaternary Science Reviews* 33, 87-99.
- Le Maitre, R.W., Bateman, P., Dudek, A., Keller, J., Lameyre, Le Bas, M.J., Sabine, P.A., Schmid, R., Sorensen, H., Streckeisen, A., Woolley, A.R., Zanettin, B., 1989. *A Classification of Igneous Rocks and Glossary of Terms*. Blackwell, Oxford.
- Lowe, D.J., 2011. Tephrochronology and its application: A review. *Quaternary Geochronology* 6, 107-153.
- MacDonald, G.A., Katsura, T. 1964. Chemical composition of Hawaiian lavas. *Journal of Petrology* 5, 83-133.
- MacLeod, A., Matthews, I.P., Lowe, J.J., Palmer, A.P., Albert, P.G., 2015. A second tephra isochron for the Younger Dryas period in northern Europe: The Abernethy Tephra. *Quaternary Geochronology* 28, 1-11.
- Martrat, B., Grimalt, J.O., Shackleton, N.J., de Abreu, L., Hutterli, M.A. and Stocker, T.F., 2007. Four climate cycles of recurring deep and surface water destabilizations on the Iberian Margin. *Science* 317, 502-507.
- Matthews, I.P., Birks, H.H., Bourne, A.J., Brooks, S.J., Lowe, J.J., MacLeod, A., Pyne-O'Donnell, S.D.F., 2011. New age estimates and climatostratigraphic correlations for the Borrobol and Penifiler Tephra: evidence from Abernethy Forest, Scotland. *Journal of Quaternary Science* 26, 247-252.

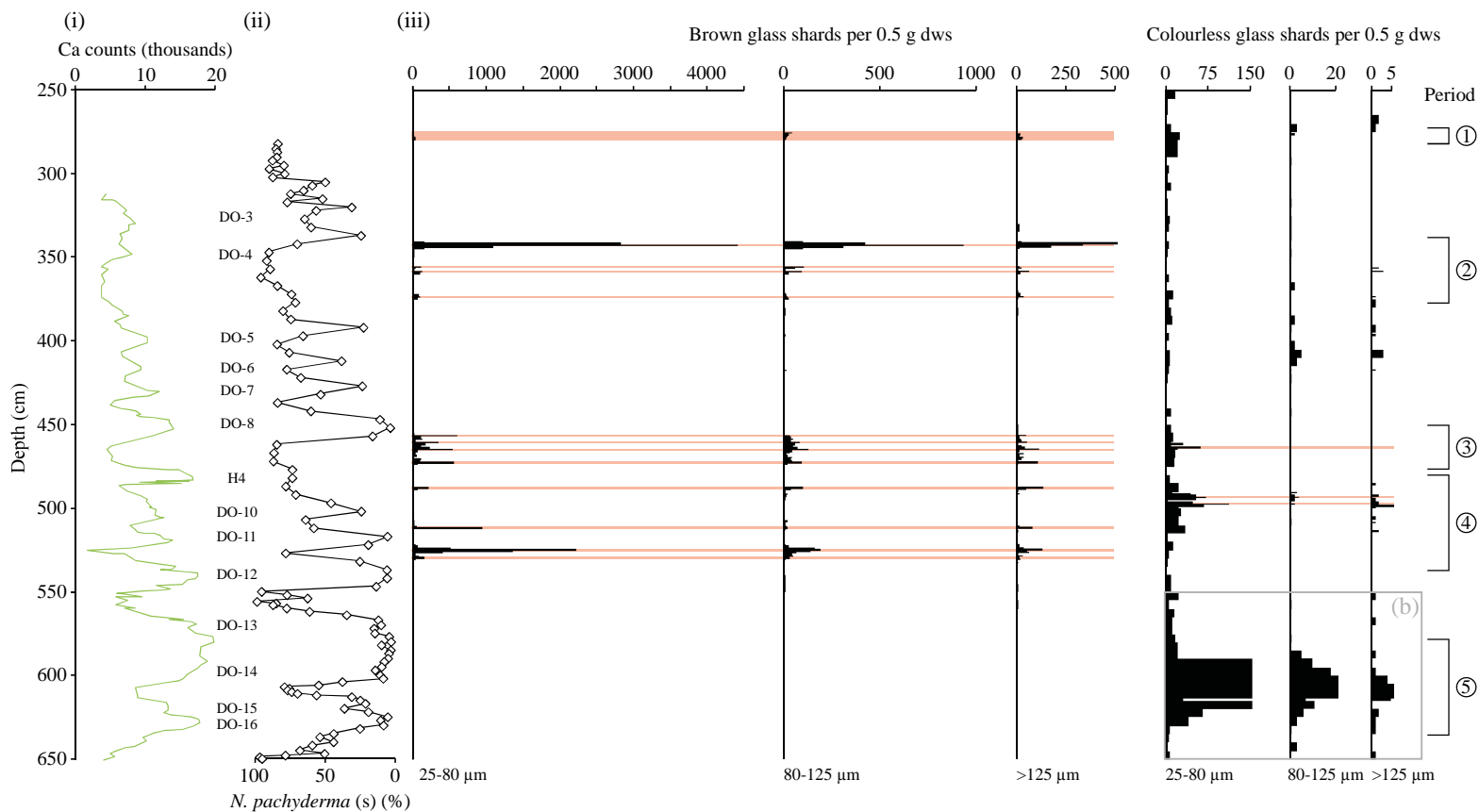
- Matthews, I.P., Trincardi, F., Lowe, J.J., Bourne, A.J., Macleod, A., Abbott, P.M., Andersen, N., Asioli, A., Blockley, S.P.E., Lane, C.S., Oh, Y.A., Satow, C.S., Staff, R.A., Wulf, S., 2015. Developing a robust tephrochronological framework for Late Quaternary marine records in the Southern Adriatic Sea: new data from core station SA03-11. *Quaternary Science Reviews* 118, 84-104.
- Newnham, R.M., Lowe, D.J., 1999. Testing the synchronicity of pollen signals using tephrostratigraphy. *Global and Planetary Change* 21, 113-128.
- Newnham, R.M., Lowe, D.J., Green, J.D., Turner, G.M., Harper, M.A., McGlone, M.S., Stout, S.L., Horie, S., Froggatt, P.C., 2004. A discontinuous ca. 80 ka record of Late Quaternary environmental change from Lake Omapere, Northland, New Zealand. *Palaeogeography, Palaeoclimatology, Palaeoecology* 207, 165-198.
- North Greenland Ice Core Project Members, 2004. High-resolution record of Northern Hemisphere climate extending into the last interglacial period. *Nature* 431, 147-151.
- Óladóttir, B.A., Sigmarsson, O., Larsen, G., Devidal, J.-L., 2011. Provenance of basaltic tephra from Vatnajökull volcanoes, Iceland, as determined by major- and trace-element analyses. *The Holocene* 21, 1037-1048.
- Pearce, N.J.G., Abbott, P.M., Martin-Jones, C., 2014. Microbeam methods for the analysis of glass in fine grained tephra deposits: a SMART perspective on current and future trends. In Austin, W.E.N., Abbott, P.M., Davies, S.M., Pearce, N.J.G., Wastegård, S., (eds) *Marine Tephrochronology*, Geological Society of London Special Publication 398, 29-46.
- Pearce, N.J.G., Bendall, C.A., Westgate, J.A., 2008. Comment on “Some numerical considerations in the geochemical analysis of distal microtephra” by A.M. Pollard, S.P.E. Blockley and C.S. Lane. *Applied Geochemistry* 23, 1353-1364.
- Pearce, N.J.G., Denton, J.S., Perkins, W.T., Westgate, J.A., Alloway, B.V., 2007. Correlation and characterisation of individual glass shards from tephra deposits using trace element laser ablation ICP-MS analyses: current status and future potential. *Journal of Quaternary Science* 22, 721-736.
- Pearce N.J.G., Perkins W.T., Westgate J.A., Gorton M.P., Jackson S.E., Neal C.R., Chenery S.P., 1997. A compilation of new and published major and trace element data for NIST SRM 610 and NIST SRM 612 glass reference materials. *Geostandards Newsletter* 21, 115-144.
- Pearce N.J.G., Perkins W.T., Westgate J.A., Wade S.C., 2011. Trace-element microanalysis by LA-ICP-MS: the quest for comprehensive chemical characterisation of single, sub-10 µm volcanic glass shards. *Quaternary International* 246, 57-81.
- Perkins M.E., Brown F.H., Nash W.P., McIntosh W., Williams S.K., 1998. Sequence, age, and source of silicic fallout tuffs in middle to late Miocene basins of the northern Basin and Range province. *Bulletin of the Geological Society of America* 110, 344-360.

- Perkins M.E., Nash W.P., Brown F.H., Fleck R.J., 1995. Fallout tuffs of Trapper Creek, Idaho – a record of Miocene explosive volcanism in the Snake River Plain volcanic province. *Bulletin of the Geological Society of America* 107, 1484-1506.
- Pilcher, J., Bradley, R.S., Francus, P., Anderson, L., 2005. A Holocene tephra record from the Lofoten Islands, Arctic Norway. *Boreas* 34, 136-156.
- Rasmussen, S.O., Bigler, M., Blockley, S.P., Blunier, T., Buchardt, S.L., Clausen, H.B., Cvijanovic, I., Dahl-Jensen, D., Johnsen, S.J., Fischer, H., Gkinis, V., Guillevic, M., Hoek, W.Z., Lowe, J.J., Pedro, J.B., Popp, T., Seierstad, I.K., Steffensen, J.P., Svensson, A.M., Vallelonga, P., Vinther, B.M., Walker, M.J., Wheatley, J.J., Winstrup, M., 2014. A stratigraphic framework for abrupt climatic changes during the Last Glacial period based on three synchronized Greenland ice-core records. *Quaternary Science Reviews* 106, 14-28.
- Sanchez Goñi, M.F., Harrison, S.P., 2010. Millennial-scale climate variability and vegetation changes during the Last Glacial: Concepts and terminology. *Quaternary Science Reviews* 29, 2823-2827.
- Scourse, J.D., Hall, I.R., McCave, I.N., Young, J.R., Sugdon, C., 2000. The origin of Heinrich layers: evidence from H2 for European precursor events. *Earth and Planetary Science Letters* 182, 187-195.
- Svensson, A., Andersen, K.K., Bigler, M., Clausen, H.B., Dahl-Jensen, D., Davies, S.M., Johnsen, S.J., Muscheler, R., Parrenin, F., Rasmussen, S.O., Röthlisberger, R., Seierstad, I., Steffensen, J.P., Vinther, B.M., 2008. A 60 000 year Greenland stratigraphic ice core chronology. *Climate of the Past* 4, 47-57.
- Turney, C.S.M., 1998. Extraction of rhyolitic component of Vedde microtephra from minerogenic lake sediments. *Journal of Palaeolimnology* 19, 199-206.
- Van Kreveld, S., Sarnthein, M., Erlenkeuser, H., Grootes, P., Jung, S., Nadeau, M.J., Pflaumann, U., Voelker, A., 2000. Potential links between surging ice sheets, circulation changes, and the Dansgaard-Oeschger cycles in the Irminger Sea, 60-18 kyr. *Paleoceanography* 15, 425-442.
- Wastegård, S., Rasmussen, T.L., 2014. Faroe Marine Ash Zone IV: a new MIS 3 ash zone on the Faroe Islands margin. In Austin, W.E.N., Abbott, P.M., Davies, S.M., Pearce, N.J.G., Wastegård, S., (eds) *Marine Tephrochronology*, Geological Society of London Special Publication 398, 81-93.
- Wastegård, S., Rasmussen, T.L., Kuijpers, A., Nielsen, T., van Weering, T.C.E., 2006. Composition and origin of ash zones from Marine Isotope Stages 3 and 2 in the North Atlantic. *Quaternary Science Reviews* 25, 2409-2419.
- Zielinski G.A., Mayewski P.A., Meeker L.D., Gronvöld K., Germani M.S., Whitlow S., Twickler M.S., Taylor K., 1997. Volcanic aerosol records and tephrochronology of the Summit, Greenland, ice cores. *Journal of Geophysical Research* 102, 26625-26640.

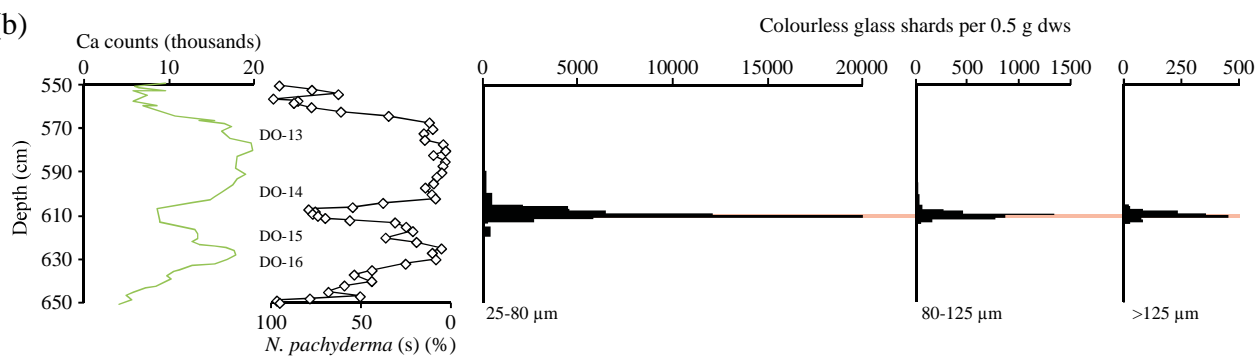
1152 Zumaque, J., Eynaud, F., Zaragosi, S., Marret, F., Matsuzaki, K.M., Kissel, C., Roche,
1153 D.M., Malaize, B., Michel, E., Billy, I., Richter, T., Palis, E., 2012. An ocean-ice
1154 coupled response during the last glacial: a view from a marine isotope stage 3 record
1155 south of the Faeroe Shetland Gateway. *Climate of the Past* 8, 1997-2017.

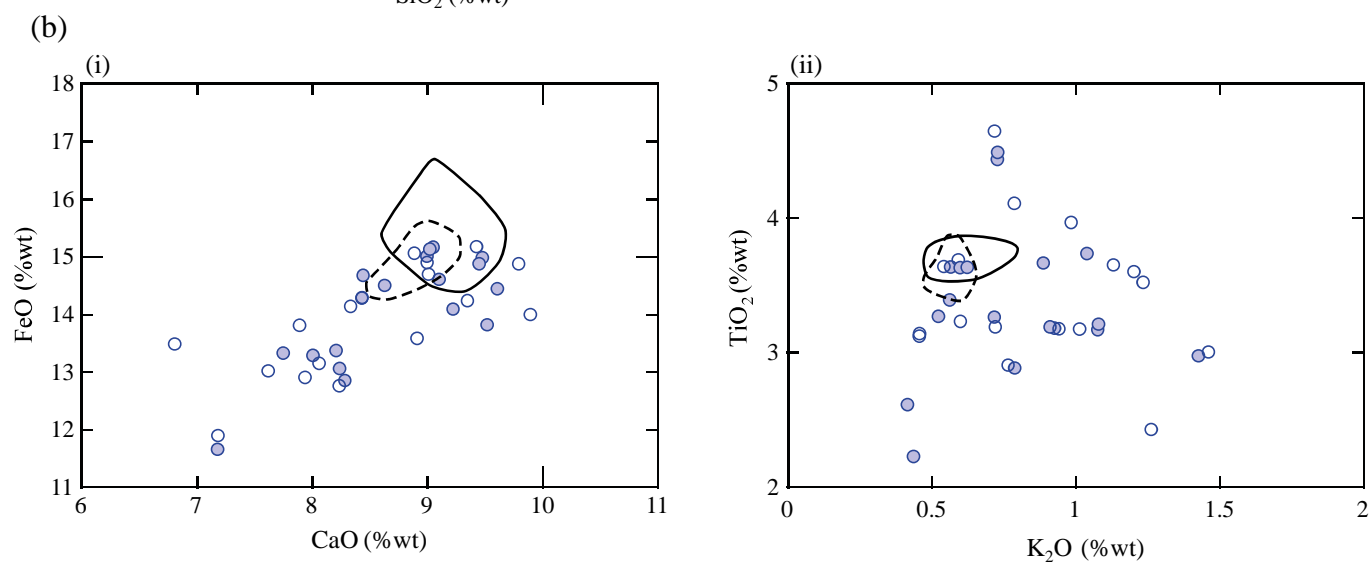
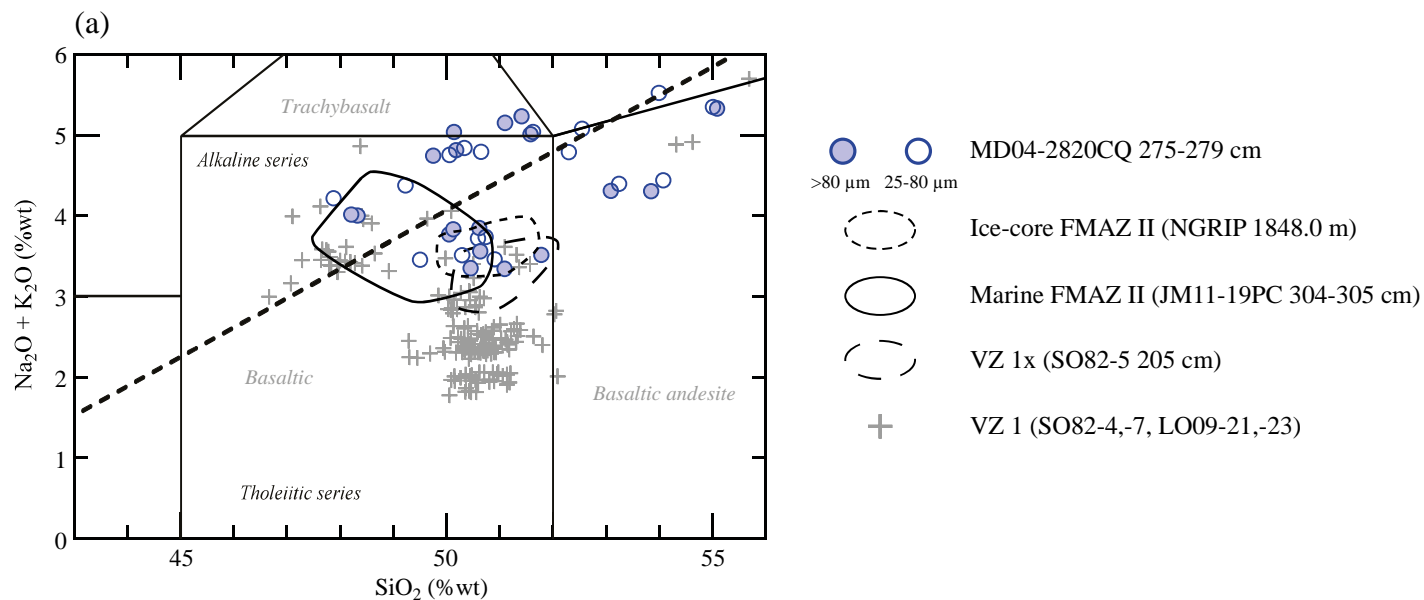


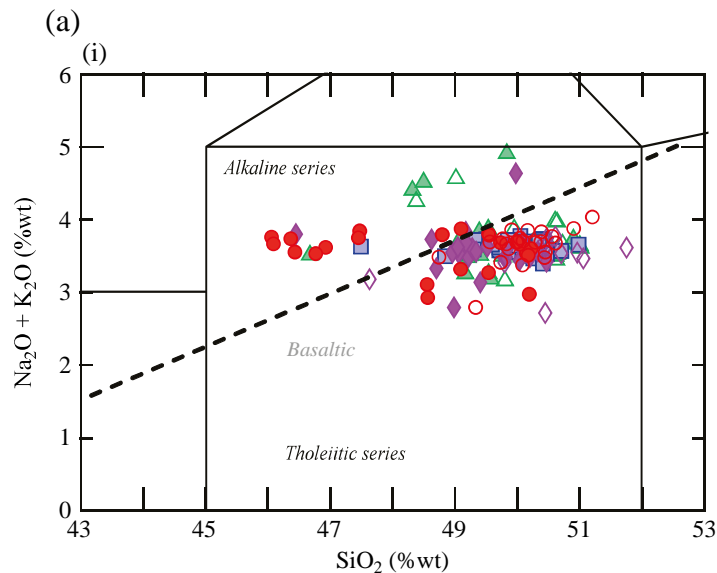
(a)



(b)



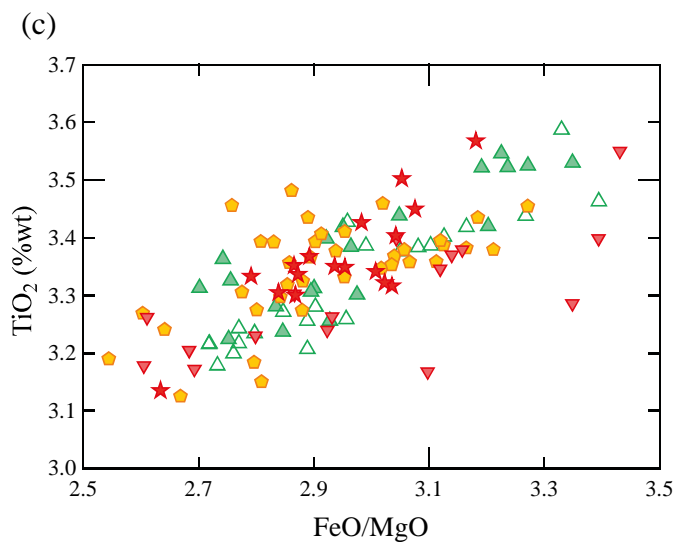
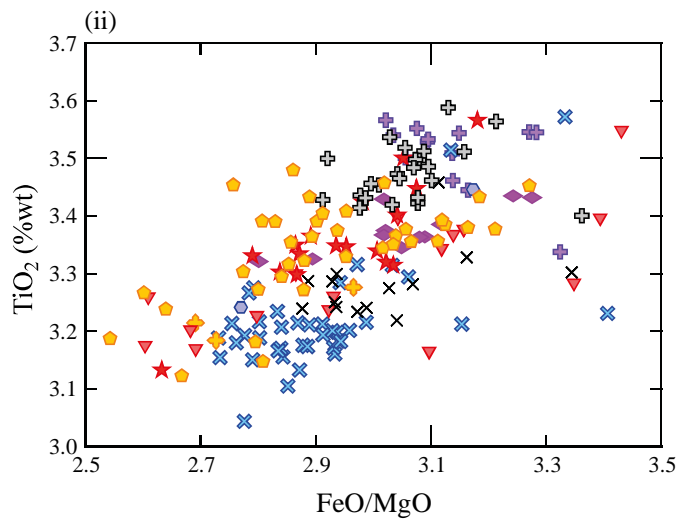
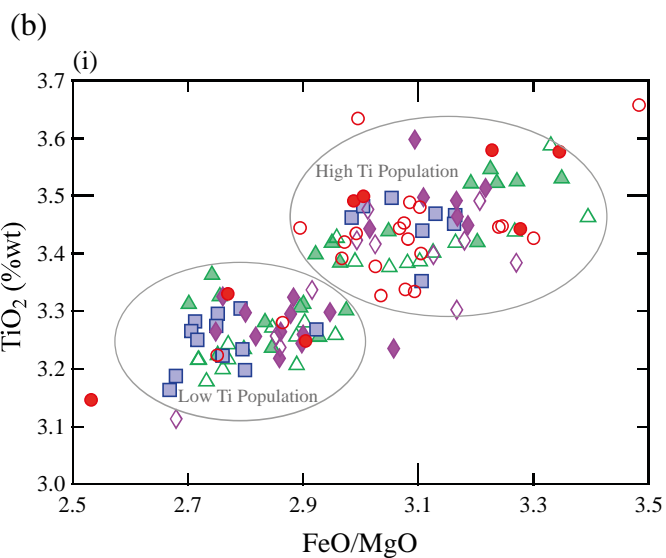
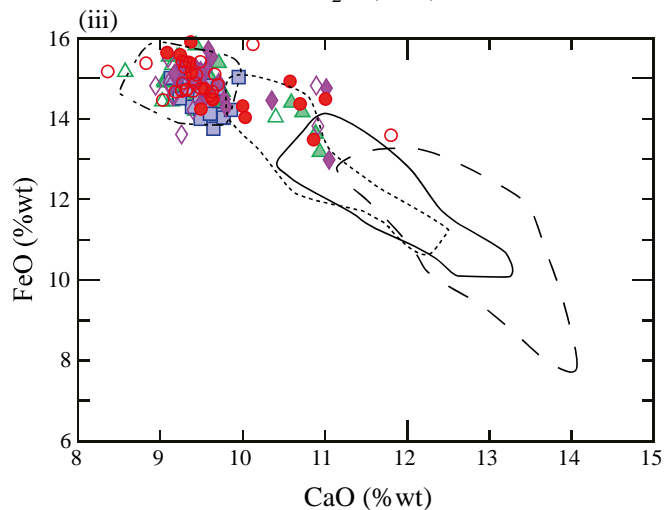
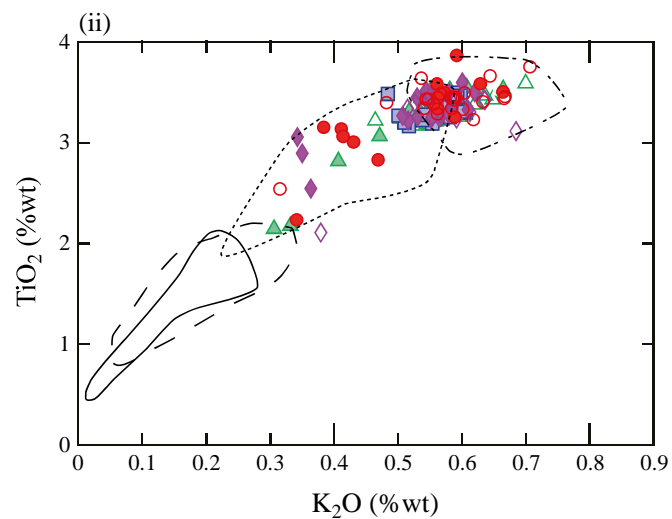




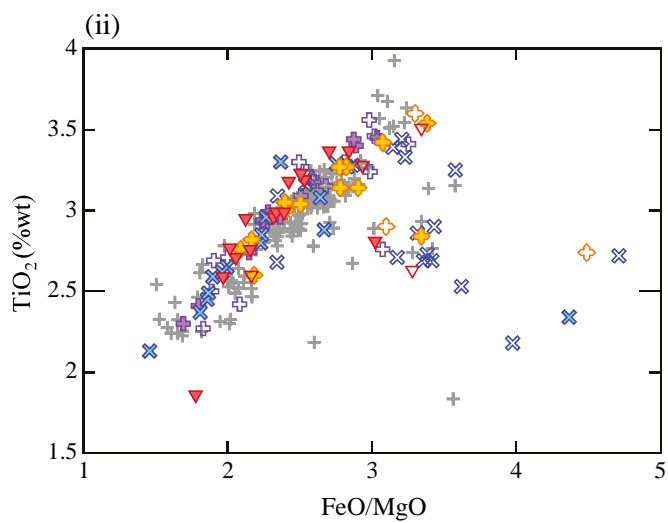
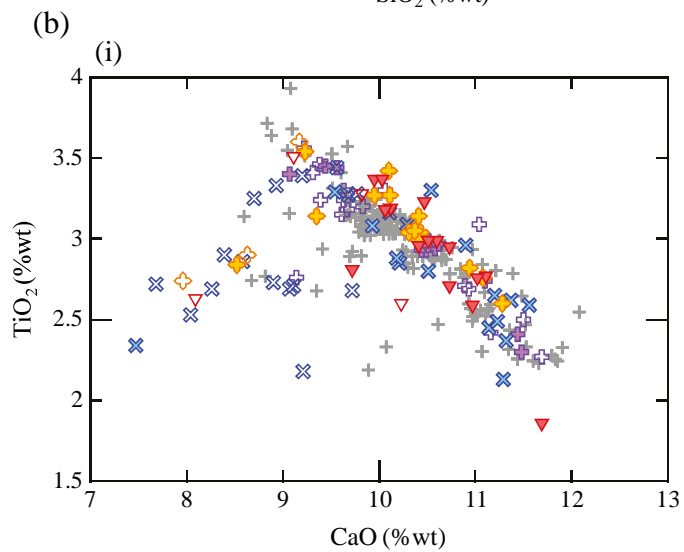
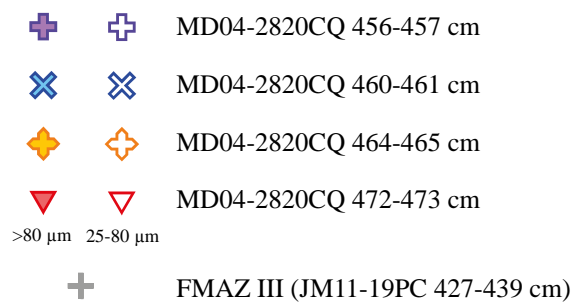
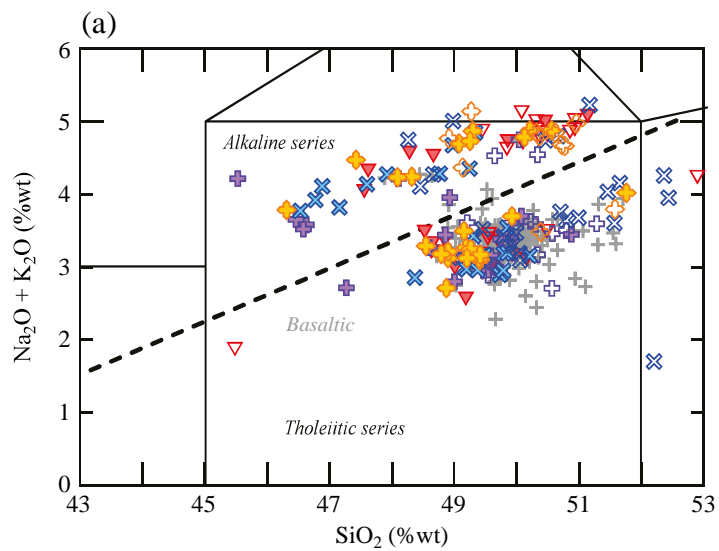
- ▲ MD04-2820CQ 342-343 cm
- MD04-2820CQ 355-356 cm
- ◆ MD04-2820CQ 358-359 cm
- MD04-2820CQ 373-374 cm

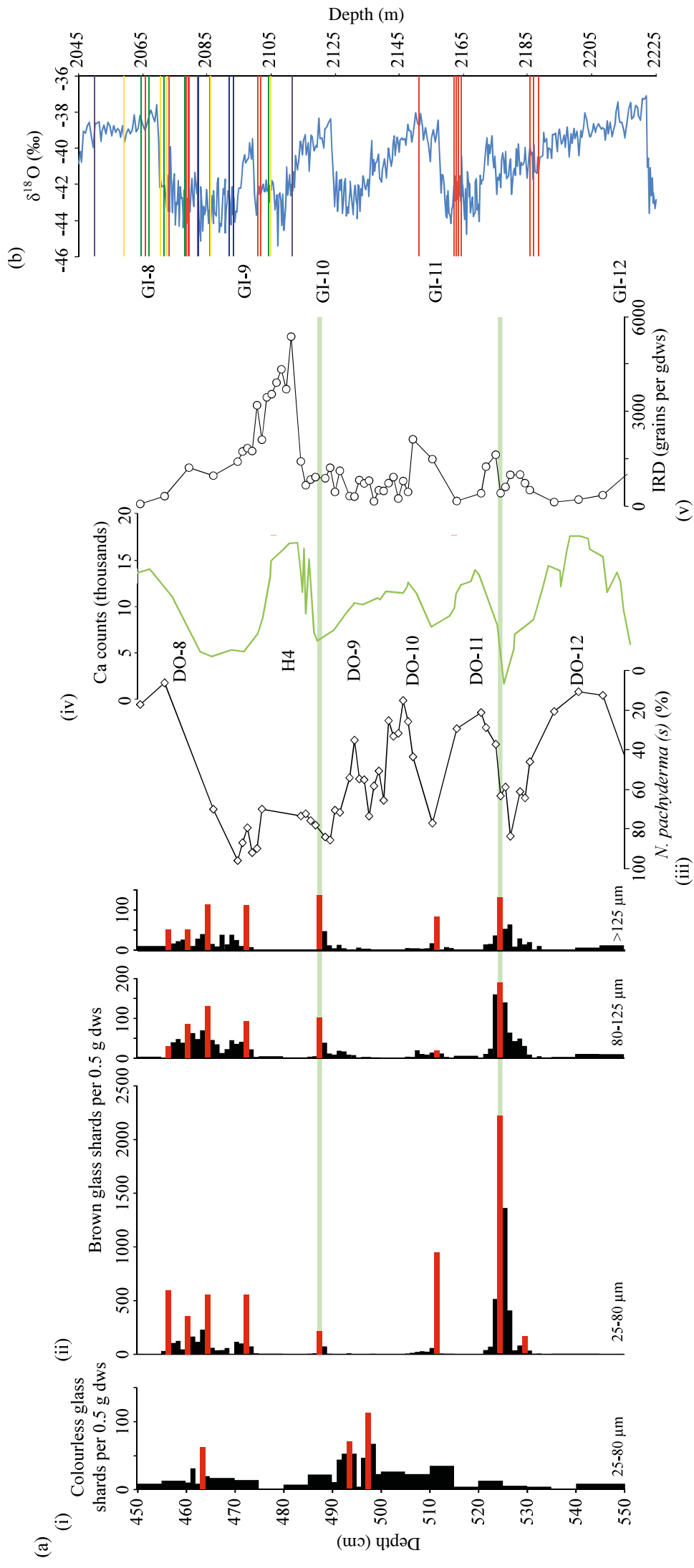
>80 μm 25-80 μm

Tholeiitic Volcanic Systems: ○ Reykjanes ○ Grímsvötn
 () Veidivötn-Bárdarbunga () Kverkfjöll

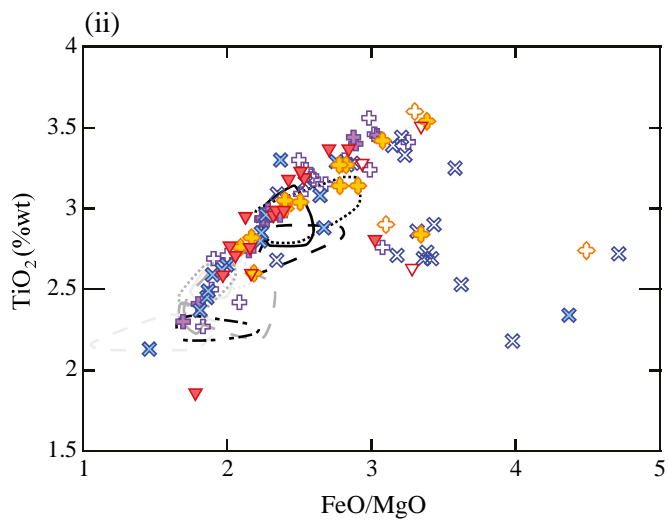
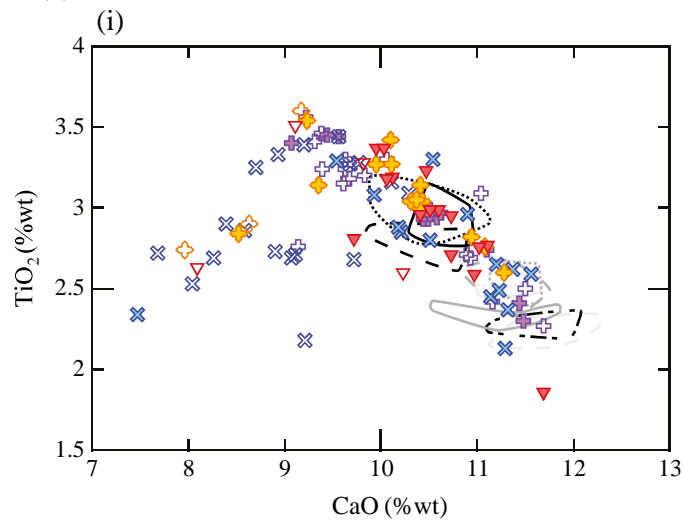


- ✚ NGRIP 1882.50 m ✚ NGRIP 1908.70 m
- ✦ GRIP 2061.40 m ▼ GRIP 2064.35 m
- ⬢ NGRIP 1913.10 m ◆ GRIP 2067.85 m
- ✕ NEEM 1671.85 m ★ NGRIP 1931.60 m
- ⊕ GRIP 2081.40 m ⬢ NGRIP 1950.50 m

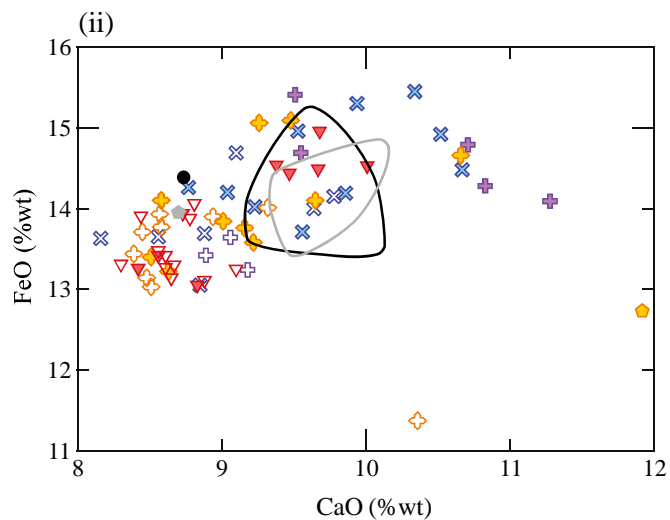
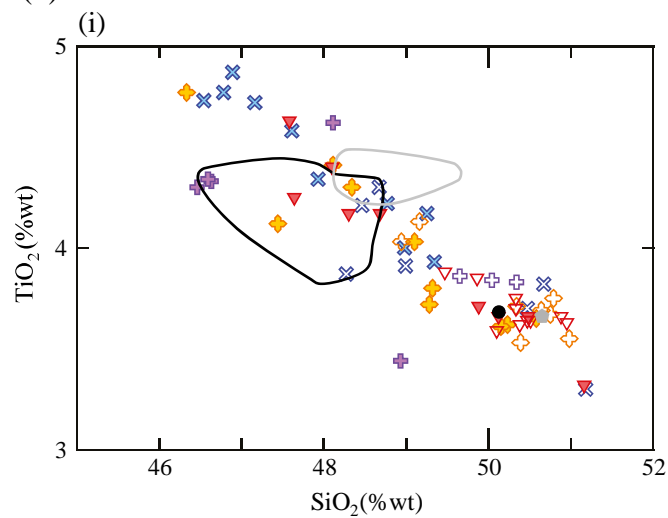
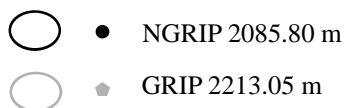


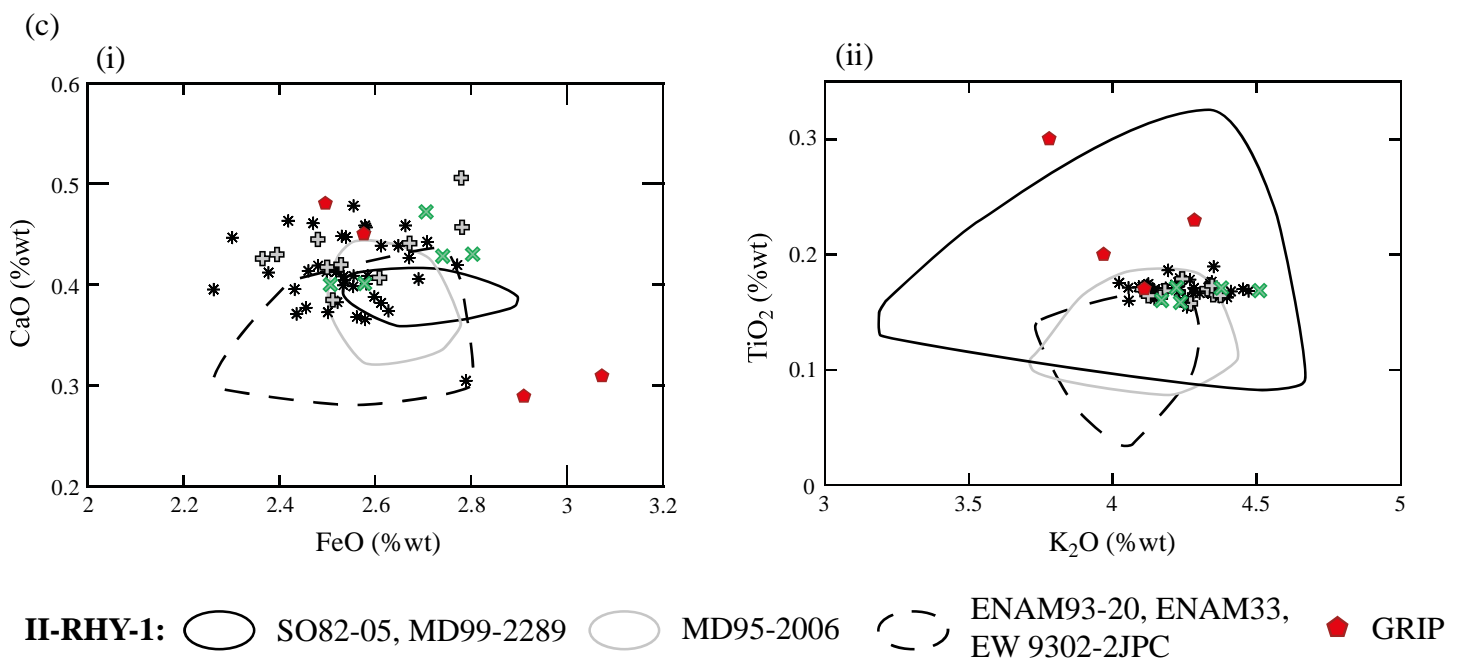
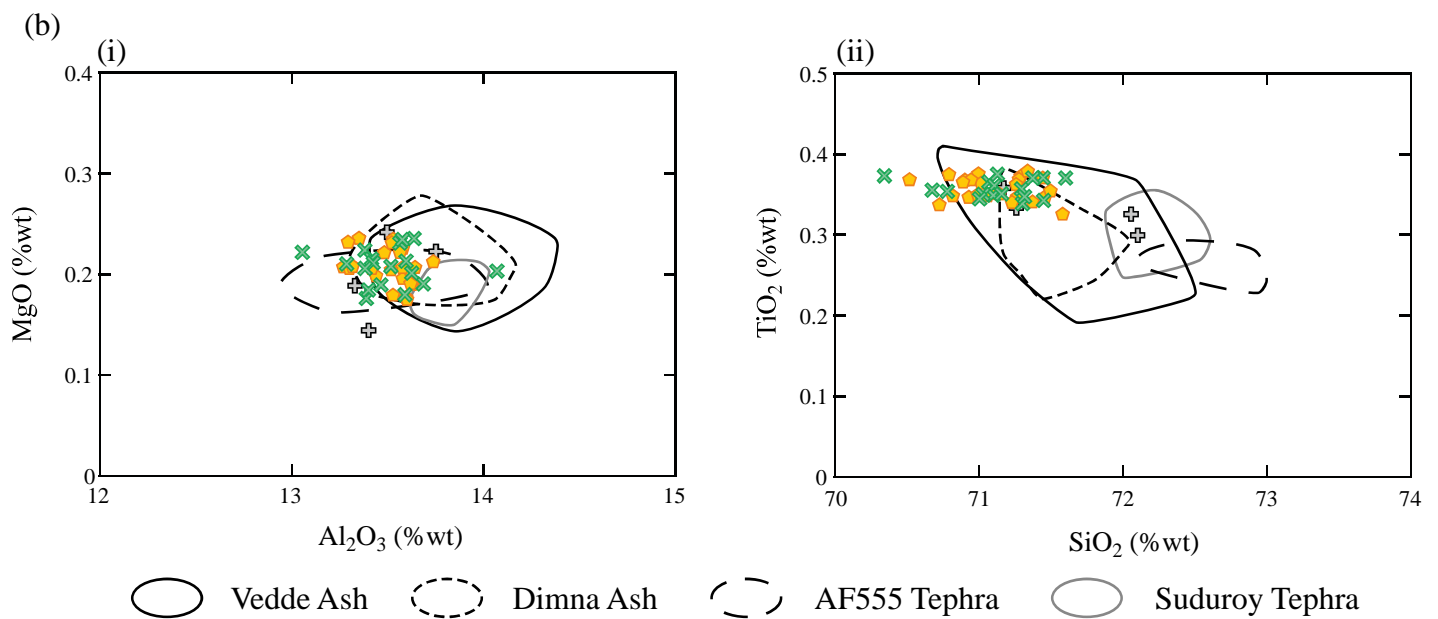
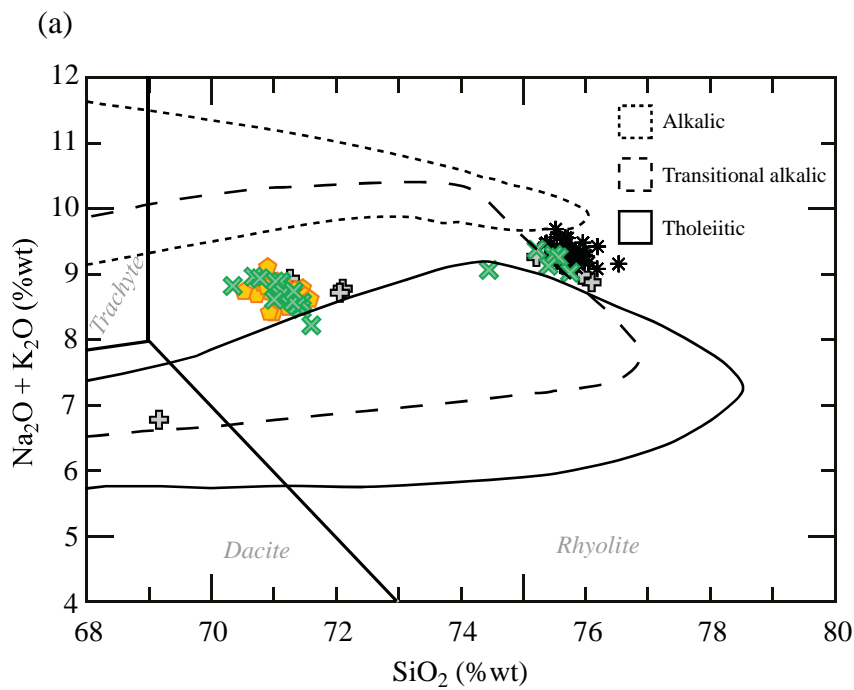


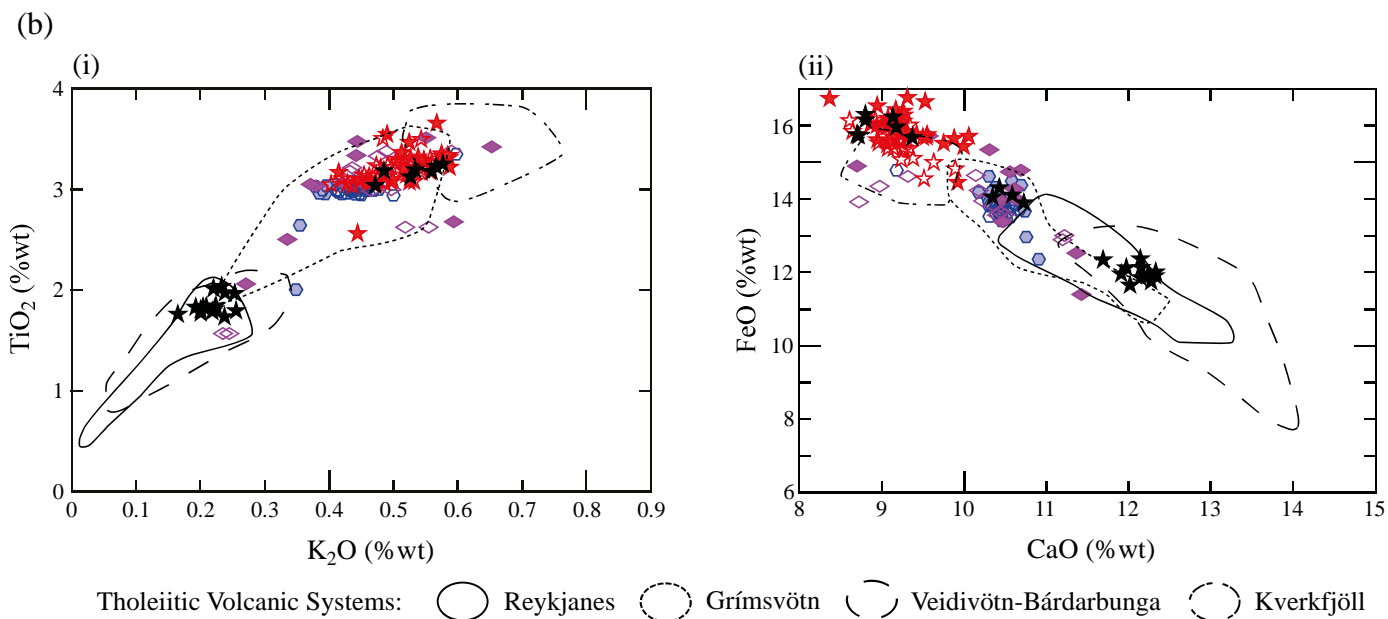
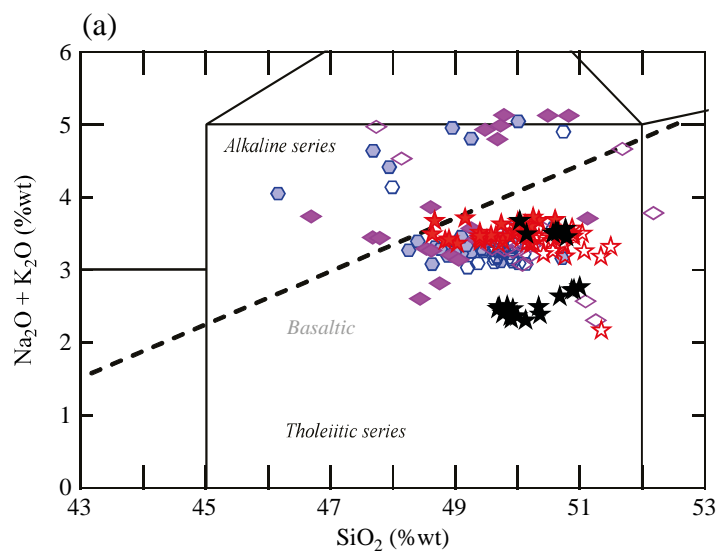
(a)



(b)

*Outliers*





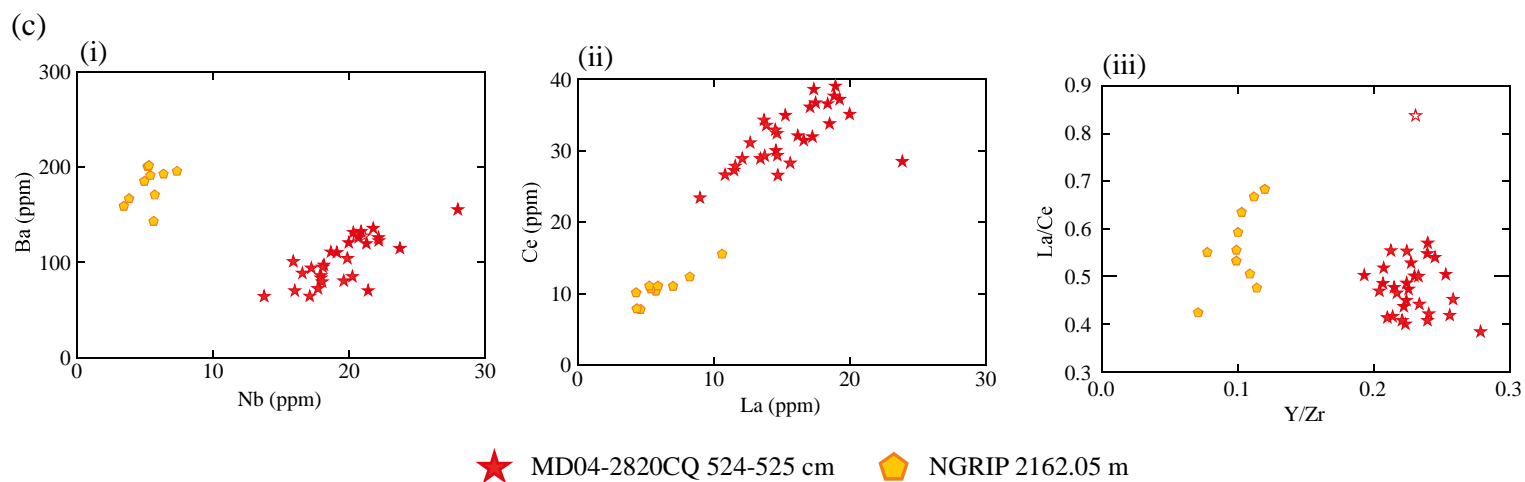
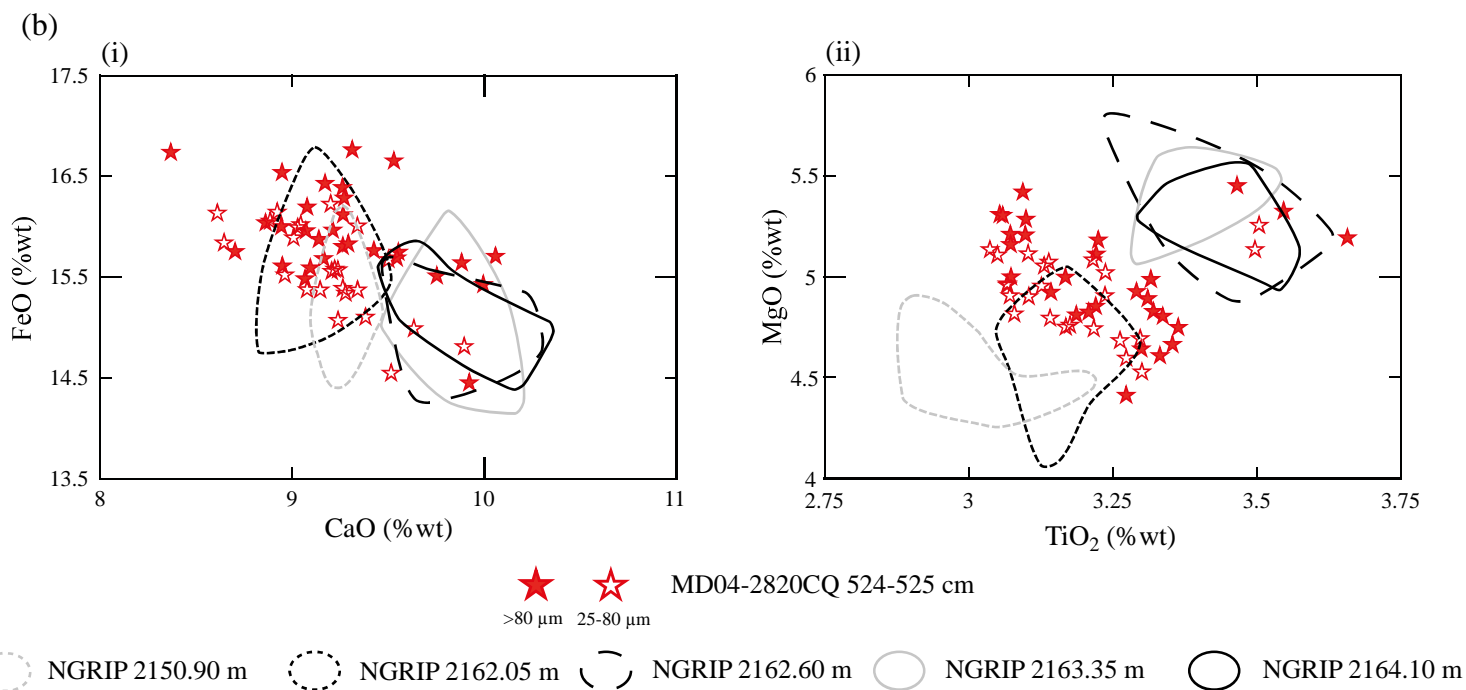
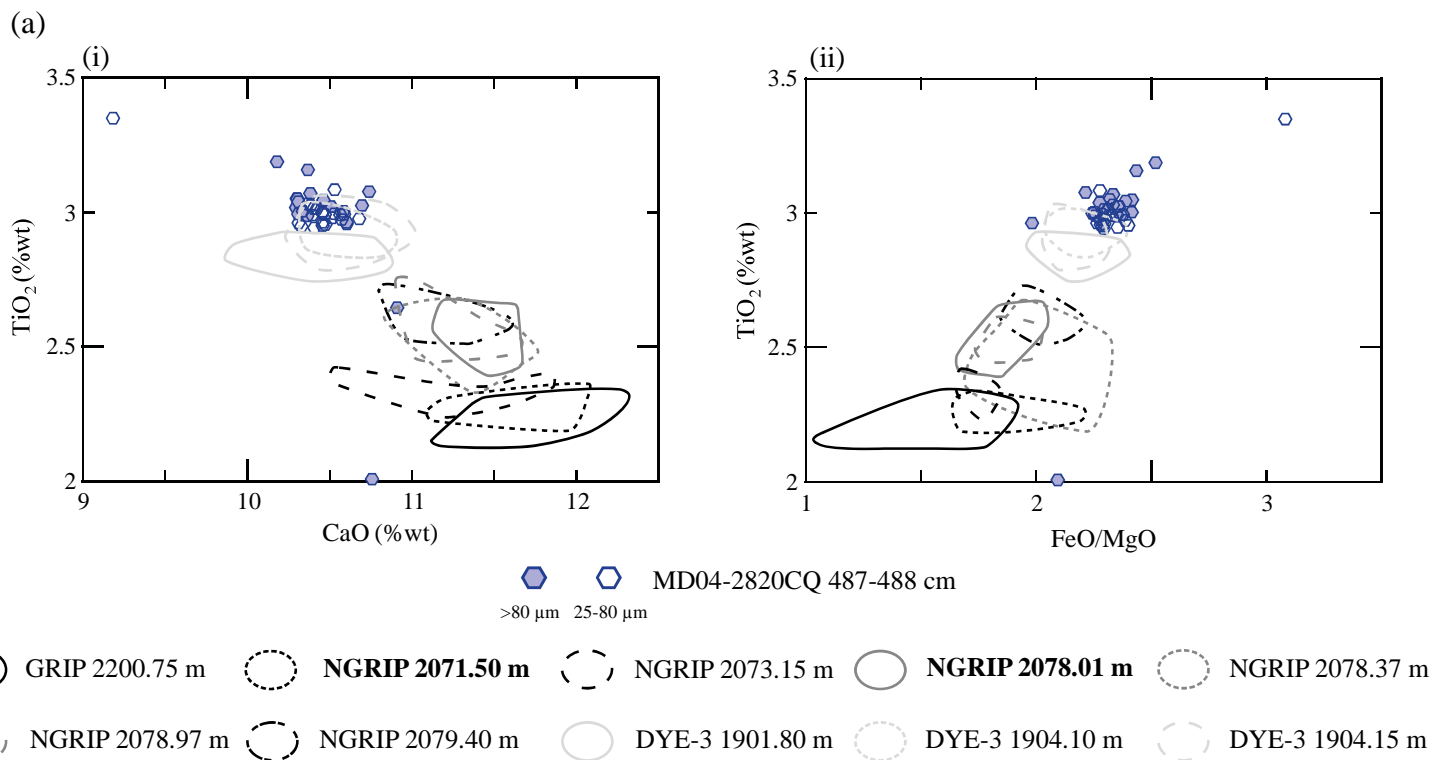


Table 1:

Ice core horizon	D ²	SC
NGRIP 2150.90 m	10.042	0.959
NGRIP 2162.05 m	1.740	0.977
NGRIP 2162.60 m	8.349	0.959
NGRIP 2163.35 m	9.709	0.953
NGRIP 2164.10 m	8.239	0.952

Table 2:

Depth Interval	Timing	Composition	Potential Source	Correlations
456-473 cm	DO-8 warming	Heterogenous Tholeiitic Basaltic	Grímsvötn, Iceland	FMAZ III*
487-488 cm	Between DO-10 and DO-9	Tholeiitic Basaltic	Grímsvötn, Iceland	New horizon
497-498 cm	DO-11	Transitional alkali Rhyolitic	Katla, Iceland	New horizon
524-525 cm	DO-11 warming	Tholeiitic Basaltic	Grímsvötn, Iceland	New horizon
610-611 cm	DO-15 cooling	Transitional alkali Rhyolitic	Tindfjallajökull, Iceland	NAAZ II